X-ray scattering and x-ray fluorescence from materials with rough interfaces

Dick K. G. de Boer
Philips Research Laboratories, Professor Holstlaan 4, 5656 AA Eindhoven, The Netherlands
(Received 18 September 1995; revised manuscript received 6 November 1995)

This paper discusses the influence of interface roughness on specular and nonspecular x-ray reflectivity and glancing-incidence x-ray fluorescence (GIXRF). Formulas are derived in the second-order distorted-wave Born approximation for samples consisting of an arbitrary number of layers. The results depend on the root-mean-square value of the interface roughness, its lateral correlation length and its degree of perpendicular correlation, as well as on the degree of jaggedness. Either flat interfaces or graded interfaces can be used as a starting point. It is shown that for GIXRF the latter approach is better. The consequences for diffuse scattering are discussed. Examples are given of calculations of specular reflectivity and GIXRF for layered materials.

I. INTRODUCTION

As we discussed in previous publications,[1,2] various complementary glancing-incidence x-ray analysis measurements exist, viz., specular reflectivity, diffuse scattering (i.e., nonspecular reflectivity), and glancing-incidence x-ray fluorescence (GIXRF), which are well suited to nondestructive depth profiling of thin-layered materials. They yield detailed information on layer thickness and composition, as well as on various aspects of interface roughness. The possible manifestations of surface roughness of single surfaces in these measurements have already been discussed in detail.[3,4]

The present paper concentrates on the theory of x-ray scattering from layered samples with rough interfaces. As the framework of the theory, we will use the distorted-wave Born approximation (DWBA).[3,5–7] In most previous publications this approximation has been applied using flat interfaces as a starting point. This approach will be used in Sec. II to work out formulas for calculating diffuse scattering (Sec. II A), specular reflection (Sec. II B), and GIXRF (Sec. II C), if necessary up to second order in the DWBA. In Sec. III we will extend the theory in a simple way to the more realistic case in which graded interfaces, obtained by laterally averaging the interface roughness, are used as a starting point. It will be shown that, for GIXRF, this approach yields better results than that using flat interfaces as a starting point. The consequences for diffuse scattering will be discussed. In Sec. IV examples will be given of calculations of specular reflection and GIXRF for layered materials. In Sec. V conclusions will be presented.

II. FLAT INTERFACES AS A STARTING POINT

In the theoretical treatment of x-ray scattering at glancing angles from a sample with rough interfaces, we will use the DWBA, which implies that we will use the wave fields for a sample with smooth interfaces as a starting point and that we will regard the roughness as a perturbation.

We will not consider explicitly the polarization of the x rays, which is justified for short wavelengths at glancing angles (cf. Ref. 1). Then the electric field ϕ obeys the Helmholtz equation

$$\nabla^2\phi+|\mathbf{k}|^2\phi-V\phi=0, \tag{1}$$

where $\mathbf{k}$ is the wave vector in vacuum and V describes the interaction with the material, e.g., $V=|\mathbf{k}|^2(1-n^2)$, for a homogeneous material with a refractive index n. We will assume that the perpendicular wave vector is much smaller than the inverse atomic distances, which implies that atomic structure may be neglected.

If the average interfaces are all parallel, V can be split into a part $V_0(z)$ which has no lateral dependence and a part $V_1(\mathbf{r})$ depending on the local position of the interfaces:

$$V(\mathbf{r})=V_0(z)+V_1(\mathbf{r}),$$

where z is the direction perpendicular to the smooth interfaces (cf. Fig. 1). We will assume that the solutions $\phi_{\mathbf{k}}^{(0)}(\mathbf{r})$ of Eq. (1) for $V_0(z)$ are known:

$$\phi_{\mathbf{k}}^{(0)}(\mathbf{r})=\psi_k(z)\exp(i\mathbf{k}_\parallel\cdot\mathbf{x}), \tag{2}$$

where $\psi_k(z)$ depends only on the perpendicular component of $\mathbf{k}$, whereas $\mathbf{k}_\parallel$ and $\mathbf{x}=(x,y)$ are the projections of $\mathbf{k}$ and the position vector $\mathbf{r}$ parallel to the surface, respectively. The perpendicular component of $\mathbf{k}$ in vacuum is $k_0=(\mathbf{k}^2-\mathbf{k}_\parallel^2)^{1/2}$.

We will treat $V_1(\mathbf{r})$ as a perturbation on $V_0(z)$. The solutions of Eq. (1) can then be written as

$$\phi_{\mathbf{k}}(\mathbf{r})=\phi_{\mathbf{k}}^{(0)}(\mathbf{r})+\phi_{\mathbf{k}}^{(1)}(\mathbf{r})+\phi_{\mathbf{k}}^{(2)}(\mathbf{r})+\cdots,$$

with $\phi_{\mathbf{k}}^{(0)}(\mathbf{r})$ being given by Eq. (2) and for $n>0$,[8]

$$\phi_{\mathbf{k}}^{(n)}(\mathbf{r})=\int d^3\mathbf{r}'\,G(\mathbf{r},\mathbf{r}')V_1(\mathbf{r}')\phi_{\mathbf{k}}^{(n-1)}(\mathbf{r}').$$

The Green's function $G(\mathbf{r},\mathbf{r}')$ can be expressed as a Fourier integral parallel to the surface:

$$G(\mathbf{r},\mathbf{r}')=\frac{1}{4\pi^2}\int d^2\mathbf{p}_\parallel\exp[i\mathbf{p}_\parallel\cdot(\mathbf{x}-\mathbf{x}')]g_p(z,z'),$$

where the integral is over all possible parallel wave vectors[9] and $g_p(z,z')$ is the one-dimensional Green's function perpendicular to the surface. It can be written as[8]

$$g_p(z,z')=-\psi_p(z_<)\psi_{\bar{p}}(z_>)/W_p,$$

where $z_<=\min(z,z')$, $z_>=\max(z,z')$, and $W_p\equiv\psi_{\bar{p}}d\psi_p/dz-\psi_p d\psi_{\bar{p}}/dz$ (the so-called Wronskian). The subscripts p

 © 1996 The American Physical Society

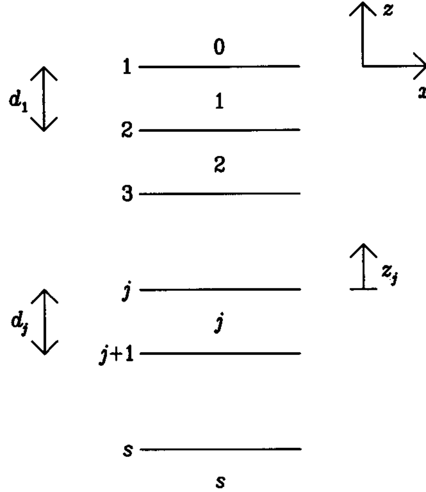

FIG. 1. Multilayer consisting of $s-1$ layers on a substrate s. Layer j has a thickness d_j, and interface j separates layers $j-1$ and j. The incoming beam is in medium 0. The y axis is perpendicular to the plane of drawing.

and $\bar{p}$ denote perpendicular wave vectors which in vacuum are directed toward and away from the top surface, respectively.

If $V_0(z)=0$ (free space) were to be taken for the unperturbed state, we would be in the Born approximation and the whole sample would be seen as a perturbation. A better approximation is to take $V_0(z)$ to correspond to the sample with flat interfaces. For a sample with one interface, this case has already been discussed by Sinha *et al.*[5] and by the present author.[3] For a multilayer the diffuse scattering was calculated using this approach by Holý *et al.*[6] Here we will extend the theory to include second-order effects and x-ray fluorescence. An even better approximation may be that where $V_0(z)$ corresponds to the sample with a laterally averaged refractive index, which results in graded interfaces.[7] The latter case will be considered in Sec. III.

Now we will consider the case where $V_0(z)$ corresponds to a multiple-layered sample with flat interfaces (see Fig. 1): $V_0(z)=0$ for $z>0$ and, for $z<0$, in layer j, $V_0(z)=k_{cj}^2$ for $-d_j<z_j<0$, where the critical wave vector k_{cj} is defined according to $k_{cj}^2=|\mathbf{k}|^2(1-n_j^2)$, n_j is the (complex) refractive index of the material in layer j, d_j is the thickness of layer j, and $z_j\equiv z+\sum_{i=1}^{j-1}d_i$. If we start with a plane wave in vacuum ("layer" 0) with a wave vector $\mathbf{k}$, the solution of the wave equation is then Eq. (2) with, in layer j,

$$\psi_k(z_j)=E_j^{\downarrow}(k)\exp(ik_jz_j)+E_j^{\uparrow}(k)\exp(-ik_jz_j), \tag{3}$$

where $k_j=(k_0^2-k_{cj}^2)^{1/2}$ is the z component of the wave vector in material j and the amplitudes $E_j^{\downarrow}(k)$ and $E_j^{\uparrow}(k)$ are the transmitted and reflected fields, respectively, at the top of layer j, which can be obtained from a matrix formalism[10] or from a recursive formalism.[11]

In the following we also need the "irregular" solution, which is, in layer j,

$$\psi_{\bar{k}}(z_j)=E_j^{\downarrow}(\bar{k})\exp(ik_jz_j)+E_j^{\uparrow}(\bar{k})\exp(-ik_jz_j), \tag{4}$$

where $E_j^{\downarrow}(\bar{k})$ and $E_j^{\uparrow}(\bar{k})$ are the reflected and transmitted fields, respectively, at the top of layer j, for a wave starting inside the substrate s. They are obtained in a similar way as $E_j^{\downarrow}(k)$ and $E_j^{\uparrow}(k)$. Without loss of generality, we can take $E_0^{\downarrow}(k)=E_s^{\uparrow}(\bar{k})=1$. Furthermore, we have $E_s^{\uparrow}(k)=E_0^{\downarrow}(\bar{k})=0$.

Next we will consider the case where the interfaces are rough. Suppose that interface j, separating layers $j-1$ and j, has at position $\mathbf{x}$ a height deviation $h_j(\mathbf{x})$. Then $V_1(\mathbf{r})=\sum_{j=1}^{s}V^j$ and

$$V^j=k_{cj}^2-k_{c,j-1}^2 \quad \text{for } 0<z_j<h_j(\mathbf{x}) \quad \text{if } h_j(\mathbf{x})>0,$$

$$V^j=-(k_{cj}^2-k_{c,j-1}^2) \quad \text{for } h_j(\mathbf{x})<z_j<0 \quad \text{if } h_j(\mathbf{x})<0,$$

and $V^j=0$ elsewhere.

From the above it follows that, in layer j,

$$\phi_{\mathbf{k}}^{(n)}(\mathbf{r})=-\frac{1}{4\pi^2}\int\frac{d^2\mathbf{p}_\parallel}{W_p}\exp(i\mathbf{p}_\parallel\cdot\mathbf{x})\left[\psi_p(z_j)\sum_{i=1}^{j}T_i^{(n)}(\bar{p},k)+\psi_{\bar{p}}(z_j)\sum_{i=j+1}^{s}T_i^{(n)}(p,k)\right], \tag{5}$$

where the coefficients

$$T_j^{(n)}(p,k)=(k_{cj}^2-k_{c,j-1}^2)\int d^2\mathbf{x}'\,\exp(-i\mathbf{p}_\parallel\cdot\mathbf{x}')\int_0^{h_j(\mathbf{x}')}dz_j'\,\psi_p(z_j')\,\phi_{\mathbf{k}}^{(n-1)}(\mathbf{r}') \tag{6}$$

form the so-called T matrix. Substituting Eqs. (3) and (4) in the Wronskian yields $W_p=2ip_j[E_j^{\downarrow}(p)E_j^{\uparrow}(\bar{p})-E_j^{\uparrow}(p)E_j^{\downarrow}(\bar{p})]$, where p_j is the perpendicular component of $\mathbf{p}$ in layer j. The Wronskian is independent of j and can be written as, for instance, $W_p=2ip_0E_0^{\uparrow}(\bar{p})$.

Strictly speaking, expression (5) is not valid inside the interface layer [where $V_1(\mathbf{r})\neq 0$], but in Appendix A we will show that it is still valid up to $O[(k_{cj}^2-k_{c,j-1}^2)^2\sigma_j^4]$ [where σ_j is the root-mean-square (rms) roughness of interface j], which is in general sufficient. By substituting $\phi_{\mathbf{k}}^{(1)}$ in Eq. (6), we can express all higher-order T-matrix elements in the first-order elements, for instance,

$$T_j^{(2)}(k',k) = -\frac{1}{4\pi^2}\int \frac{d^2\mathbf{p}_\parallel}{W_p}\left[T_j^{(1)}(k',p)\sum_{i=1}^{j} T_i^{(1)}(\bar{p},k) + T_j^{(1)}(k',\bar{p})\sum_{i=j+1}^{s} T_i^{(1)}(p,k)\right]. \tag{7}$$

A. Diffuse scattering

To calculate both specular and nonspecular reflectivity, we will consider the perturbed wave function for $z>0$, outside the sample:

$$\phi_{\mathbf{k}}^{(n)}(\mathbf{r}) = \frac{i}{8\pi^2}\int \frac{d^2\mathbf{p}_\parallel}{p_0}\exp[i(\mathbf{p}_\parallel\cdot\mathbf{x} - p_0 z)]\sum_{i=1}^{s} T_i^{(n)}(p,k). \tag{8}$$

This expression describes waves scattered in all directions. Up to the order $n=1$, the differential cross section for scattering in the direction of $\mathbf{p}$ is

$$\frac{d\sigma(p\leftarrow k)}{d\Omega} = \frac{1}{16\pi^2}\sum_{j=1}^{s}\sum_{i=1}^{s} T_j^{(1)*}(p,k)T_i^{(1)}(p,k). \tag{9}$$

To calculate the diffuse scattering, we have to take a configurational average corresponding to all possible positions $h_j(\mathbf{x})$ of the interfaces and have to subtract the specular part (cf. Refs. 3, 5). For the specular component we have to take $\mathbf{p}_\parallel = \mathbf{k}_\parallel$ (see the following subsection).

We will calculate the T matrix, Eq. (6), by approximating the unperturbed functions for $V^j \neq 0$ by $\psi_k(z_j) \simeq E_j^{\downarrow}(k)\exp(ik_j z) + E_j^{\uparrow}(k)\exp(-ik_j z)$, also when $z_j>0$. This is reasonable for small values of k_0 up to $O(k_j^2\sigma_j^2)$ and also for large values of k_0 up to $O[(k_{cj}^2 - k_{c,j-1}^2)/k_0^2]$. Then we find

$$T_j^{(1)}(p,k) \simeq (k_{cj}^2 - k_{c,j-1}^2)[E_j^{\downarrow}(p)E_j^{\downarrow}(k)F_j(\mathbf{p}_\parallel - \mathbf{k}_\parallel, p_j + k_j) + E_j^{\downarrow}(p)E_j^{\uparrow}(k)F_j(\mathbf{p}_\parallel - \mathbf{k}_\parallel, p_j - k_j) + E_j^{\uparrow}(p)E_j^{\downarrow}(k)F_j(\mathbf{p}_\parallel - \mathbf{k}_\parallel, -p_j + k_j)$$
$$+ E_j^{\uparrow}(p)E_j^{\uparrow}(k)F_j(\mathbf{p}_\parallel - \mathbf{k}_\parallel, -p_j - k_j)], \tag{10}$$

with

$$F_j(\mathbf{q}_\parallel, q) \equiv -i/q\int d^2\mathbf{x}\,\exp(i\mathbf{q}_\parallel\cdot\mathbf{x})\{\exp[iqh_j(\mathbf{x})] - 1\},$$

where $\mathbf{q}_\parallel = \mathbf{p}_\parallel - \mathbf{k}_\parallel$ is the parallel wave-vector transfer.

We will calculate configurational averages (indicated by $\langle\ \rangle$) by assuming that h_j is a Gaussian random variable with a standard deviation σ_j, i.e., the rms roughness. We find

$$\langle T_j^{(1)}(p,k)\rangle = \delta_{\mathbf{p}_\parallel,\mathbf{k}_\parallel}(k_{cj}^2 - k_{c,j-1}^2)[E_j^{\downarrow}(p)E_j^{\downarrow}(k) - E_j^{\uparrow}(p)E_j^{\uparrow}(k)]\langle F_j(\mathbf{p}_\parallel - \mathbf{k}_\parallel, p_j + k_j)\rangle, \tag{11}$$

with

$$\langle F_j(\mathbf{q}_\parallel, q)\rangle = -iA\,\delta_{\mathbf{q}_\parallel,0}[\exp(-q^2\sigma_j^2/2) - 1]/q,$$

where A is the irradiated detected sample surface area.

In the evaluation of the diffuse scattering, we have to evaluate averages like

$$\langle F_j^*(\mathbf{q}_\parallel, q_j)F_i(\mathbf{q}_\parallel, q_i)\rangle - \langle F_j^*(\mathbf{q}_\parallel, q_j)\rangle\langle F_i(\mathbf{q}_\parallel, q_i)\rangle = AS_{ji}(\mathbf{q}_\parallel; q_j, q_i),$$

where

$$S_{ji}(\mathbf{q}_\parallel; q_j, q_i) \equiv \frac{\exp[-(q_j^{*2}\sigma_j^2 + q_i^2\sigma_i^2)/2]}{q_j^* q_i}\int d^2\mathbf{X}\{\exp[q_j^* q_i C_{ji}(\mathbf{X})] - 1\}\exp(i\mathbf{q}_\parallel\cdot\mathbf{X}) \tag{12}$$

can be regarded as a structure factor, $\mathbf{X} = \mathbf{x} - \mathbf{x}'$, and

$$C_{ji}(\mathbf{x} - \mathbf{x}') \equiv \langle h_j(\mathbf{x})h_i(\mathbf{x}')\rangle \tag{13}$$

is the correlation function between the roughness profiles of interfaces j and i, which is assumed to be a function of the lateral distance vector $\mathbf{x} - \mathbf{x}'$ only.

We find

$$\frac{d\sigma(p\leftarrow k)}{d\Omega}=\frac{A}{16\pi^2}\sum_{j=1}^{s}\sum_{i=1}^{s}(k_{cj}^2-k_{c,j-1}^2)^*(k_{ci}^2-k_{c,i-1}^2)\{[E_j^{\downarrow *}(k)E_j^{\downarrow *}(p)E_i^{\downarrow}(k)E_i^{\downarrow}(p)+E_j^{\uparrow *}(k)E_j^{\uparrow *}(p)E_i^{\uparrow}(k)E_i^{\uparrow}(p)]S_{ji}(\mathbf{p}_\parallel-\mathbf{k}_\parallel;k_j+p_j,k_i+p_i)+[E_j^{\downarrow *}(k)E_j^{\downarrow *}(p)E_i^{\uparrow}(k)E_i^{\uparrow}(p)+E_j^{\uparrow *}(k)E_j^{\uparrow *}(p)E_i^{\downarrow}(k)E_i^{\downarrow}(p)]S_{ji}(\mathbf{p}_\parallel-\mathbf{k}_\parallel;k_j+p_j,-k_i-p_i)$$
$$+[E_j^{\downarrow *}(k)E_j^{\downarrow *}(p)E_i^{\downarrow}(k)E_i^{\uparrow}(p)+E_j^{\uparrow *}(k)E_j^{\uparrow *}(p)E_i^{\uparrow}(k)E_i^{\downarrow}(p)]S_{ji}(\mathbf{p}_\parallel-\mathbf{k}_\parallel;k_j+p_j,k_i-p_i)$$
$$+[E_j^{\downarrow *}(k)E_j^{\downarrow *}(p)E_i^{\uparrow}(k)E_i^{\downarrow}(p)+E_j^{\uparrow *}(k)E_j^{\uparrow *}(p)E_i^{\downarrow}(k)E_i^{\uparrow}(p)]S_{ji}(\mathbf{p}_\parallel-\mathbf{k}_\parallel;k_j+p_j,-k_i+p_i)$$
$$+[E_j^{\downarrow *}(k)E_j^{\uparrow *}(p)E_i^{\downarrow}(k)E_i^{\downarrow}(p)+E_j^{\uparrow *}(k)E_j^{\downarrow *}(p)E_i^{\uparrow}(k)E_i^{\uparrow}(p)]S_{ji}(\mathbf{p}_\parallel-\mathbf{k}_\parallel;k_j-p_j,k_i+p_i)$$
$$+[E_j^{\downarrow *}(k)E_j^{\uparrow *}(p)E_i^{\uparrow}(k)E_i^{\uparrow}(p)+E_j^{\uparrow *}(k)E_j^{\downarrow *}(p)E_i^{\downarrow}(k)E_i^{\downarrow}(p)]S_{ji}(\mathbf{p}_\parallel-\mathbf{k}_\parallel;k_j-p_j,-k_i-p_i)$$
$$+[E_j^{\downarrow *}(k)E_j^{\uparrow *}(p)E_i^{\downarrow}(k)E_i^{\uparrow}(p)+E_j^{\uparrow *}(k)E_j^{\downarrow *}(p)E_i^{\uparrow}(k)E_i^{\downarrow}(p)]S_{ji}(\mathbf{p}_\parallel-\mathbf{k}_\parallel;k_j-p_j,k_i-p_i)$$
$$+[E_j^{\downarrow *}(k)E_j^{\uparrow *}(p)E_i^{\uparrow}(k)E_i^{\downarrow}(p)+E_j^{\uparrow *}(k)E_j^{\downarrow *}(p)E_i^{\downarrow}(k)E_i^{\uparrow}(p)]S_{ji}(\mathbf{p}_\parallel-\mathbf{k}_\parallel;k_j-p_j,-k_i+p_i)\}. \tag{14}$$

This expression was published for the first time by Holý *et al.*[6]

If $k_j\sigma_j$ is small, $S_{ji}(\mathbf{q}_\parallel;q_j,q_i)\simeq\tilde{C}_{ji}(\mathbf{q}_\parallel)$, where

$$\tilde{C}_{ji}(\mathbf{q}_\parallel)\equiv\int d^2\mathbf{X}\,\exp(i\mathbf{q}_\parallel\cdot\mathbf{X})C_{ji}(\mathbf{X}). \tag{15}$$

Then Eq. (14) can be greatly simplified. However, Eq. (14) is also valid for large values of $k_j\sigma_j$, provided that $k_0^2/(k_{cj}^2-k_{c,j-1}^2)\gg 1$, as is apparent from the above approximations. In that limit the result is equivalent to that of the simple Born approximation,[12] provided that the reflected fields may be neglected with respect to the downgoing fields. Note that this implies that in the case of a multilayer it is necessary to use the complete form Eq. (14) near the total-reflection area and close to Bragg peaks, whereas the Born approximation is applicable for wave vectors far from these conditions.

For the sake of completeness we mention that the diffuse transmission through a stack of layers can be found using the same method. The result is that all fields $E_j^{\downarrow}(p)$ and $E_j^{\uparrow}(p)$ have to be substituted by $E_j^{\downarrow}(\bar{p})$ and $E_j^{\uparrow}(\bar{p})$.

To be able to evaluate the diffuse scattering, we need a model for $C_{ji}(\mathbf{X})$. Spiller *et al.*[13] argued that its Fourier transform, Eq. (15), may be written as

$$\tilde{C}_{ji}(\mathbf{q}_\parallel)=\tilde{c}_{ji}^{\perp}(\mathbf{q}_\parallel)\tilde{C}_{j_>}(\mathbf{q}_\parallel), \tag{16}$$

where $j_>\equiv\max(j,i)$. As in Eq. (15), $\tilde{C}_j(\mathbf{q}_\parallel)$, the power spectral density of interface j, is the two-dimensional Fourier transform of $C_j(\mathbf{X})$, the correlation function of the roughness of interface j, whereas $\tilde{c}_{ji}^{\perp}(\mathbf{q}_\parallel)$ is the replica factor between interfaces j and i. A form frequently used for the correlation function is that introduced by Sinha *et al.*[5] for self-affine interfaces:

$$C_j(\mathbf{X})=\sigma_j^2\,\exp[-(|\mathbf{X}|/\xi_j)^{2H_j}],$$

where ξ_j is the correlation length of the roughness and the parameter H_j $(0<H_j\leqslant 1)$, describing how jagged interface j is, is connected to its fractal dimension $D_j=3-H_j$. Several other functional forms with qualitatively the same behavior have been described in the literature.[4,14] The simplest form for the replica factor is a frequency-independent one:

$$\tilde{c}_{ji}^{\perp}(\mathbf{q}_\parallel)=c_{ji}^{\perp}=\exp\left(-\sum_{n=j_<}^{j_>-1}d_n/\xi_\perp\right),$$

where $j_<\equiv\min(j,i)$ and $\xi_\perp$ is a perpendicular correlation length. A more realistic form will replicate low spatial frequencies better than higher ones.[13]

The formalism of this subsection has been successfully applied to describe diffuse-scattering measurements. Examples of such simulations can be found in Refs. 6, 15, 16.

Above, the diffuse scattering was calculated in the first-order DWBA. In Appendix B we will show that higher-order terms are smaller by a factor that is not larger than $O(k_j^2\sigma_j^2)$. In the next subsections we will show that, as for single interfaces,[3,4] the second-order contributions to specular reflectivity and GIXRF may be as strong as the first-order contributions. Higher-order terms will be smaller again by at least a factor of $O(k_j^2\sigma_j^2)$.

B. Specular reflection

Now we will proceed with the calculation of specular scattering. To do this, we have to insert, in Eq. (5), $\delta_{k_x,p_x}\delta_{k_y,p_y}\simeq(4\pi^2/A)\delta(k_x-p_x)\delta(k_y-p_y)$ and we have to take a configurational average to obtain the coherent scattering. Hence, for $n>0$, the specular component of Eq. (5) in layer 0 is

$$\phi_{\mathbf{k},\mathrm{spec}}^{(n)}(\mathbf{r})=\frac{i}{2Ak_0}\exp[i(\mathbf{k}_\parallel\cdot\mathbf{x}-k_0z)]\sum_{i=1}^{s}\langle T_i^{(n)}(k,k)\rangle.$$

When we write the specular reflection coefficient of the multilayer with rough interfaces as

$$\tilde{r}_k=r_k^{(0)}+r_k^{(1)}+r_k^{(2)}+\cdots,$$

we have $r_k^{(0)}=E_0^{\uparrow}(k)$ and, for $n>0$,

$$r_k^{(n)}=i\sum_{j=1}^{s}\langle T_j^{(n)}(k,k)\rangle/(2Ak_0). \tag{17}$$

For the sake of completeness we mention that, using the same method, we can also obtain the transmission coefficient through a multilayer stack, which

is $\tilde{t}_k = t_k^{(0)} + t_k^{(1)} + t_k^{(2)} + \cdots$ with $t_k^{(0)} = E_s^{\downarrow}(k)$ and $t_k^{(n)} = i\sum_{j=1}^{s}\langle T_j^{(n)}(\bar{k},k)\rangle/(2Ak_s)$ for $n>0$.

The first-order ($n=1$) contribution is obtained by substituting Eq. (11) with, up to $O(k_j^2\sigma_j^2)$, $\langle F_j(\mathbf{q}_\parallel,q)\rangle \simeq iA\,\delta_{\mathbf{q}_\parallel,0}q\sigma_j^2/2$. For a single surface this case can be solved self-consistently, with the result that the reflection coefficient is multiplied by the so-called Névot-Croce (NC) factor $\exp(-2k_{j-1}k_j\sigma_j^2)$.[17–19] It can be shown that for a multilayer, up to $O(k_j^2\sigma_j^2)$ and/or up to $O[(k_{cj}^2 - k_{c,j-1}^2)/k_j^2]$, the $n=1$ contribution is obtained by multiplying the reflection coefficients at each interface j by NC factors. This method is widely used for calculating reflectivities.[2]

The second-order ($n=2$) contribution is obtained by substituting Eq. (7) in Eq. (17) and taking configurational averages. It can be regarded as a sum of diffuse scattering distributions [cf. Eq. (9)], and we have to integrate over $\mathbf{p}_\parallel$ expressions as in Eq. (14). Here, however, we are not interested in the details of the shape of the diffuse scattering distribution as a function of $\mathbf{p}_\parallel$. So we can greatly simplify the calculations by proceeding up to $O(k_j^2\sigma_j^2)$, which yields, for one of the terms between brackets in Eq. (7),

$$\langle T_j^{(1)}(k',p)T_i^{(1)}(\bar{p},k)\rangle \simeq \delta_{\mathbf{k}'_\parallel,\mathbf{k}_\parallel}A(k_{cj}^2 - k_{c,j-1}^2)(k_{ci}^2 - k_{c,i-1}^2)E_j(k')E_i(k)E_j(p)E_i(\bar{p})\tilde{C}_{ji}(\mathbf{p}_\parallel - \mathbf{k}_\parallel), \tag{18}$$

with

$$E_j(k) \equiv E_j^{\downarrow}(k) + E_j^{\uparrow}(k).$$

Now Eq. (7) yields

$$\langle T_j^{(2)}(k',k)\rangle = -\delta_{\mathbf{k}'_\parallel,\mathbf{k}_\parallel}A/(4\pi^2)\sum_{i=1}^{s}(k_{cj}^2 - k_{c,j-1}^2)(k_{ci}^2 - k_{c,i-1}^2)E_j(k')E_i(k)\int d^2\mathbf{p}_\parallel/W_pE_{j_>}(p)E_{j_<}(\bar{p})\tilde{C}_{ji}(\mathbf{p}_\parallel - \mathbf{k}_\parallel). \tag{19}$$

To calculate Eq. (19), we have to evaluate the integral over $\mathbf{p}_\parallel$. This two-dimensional integral can be transformed into pole coordinates and then can be performed either numerically or (partially) analytically (cf. Ref. 3).

The second-order contribution describes the correlation between the radiation scattered from the various interfaces, which in general cannot be taken into account by using simple multiplication factors for single-interface reflection coefficients (cf. Ref. 20). This is only possible for very large values of ξ if all the layers are perfectly correlated (i.e., large $\xi_\perp$), or for very small values of ξ.

We will consider in more detail these limiting cases, which depend on the value of $(|\mathbf{k}| - |\mathbf{k}_\parallel|)\xi_j/2 \simeq k_0^2\xi_j/|\mathbf{k}|$. We found that, if this value is $\ll 1$, $\langle T_j^{(2)}(k',k)\rangle/\langle T_j^{(1)}(k',k)\rangle = O(k_0\sqrt{\xi_j/|\mathbf{k}|})$, and the first-order (or NC) result is a good approximation. If, on the other hand, $k_0^2\xi_j/|\mathbf{k}| \gg 1$, then $\tilde{C}_j(\mathbf{p}_\parallel - \mathbf{k}_\parallel)$ approaches $4\pi^2\sigma_j^2$ times a δ function centered at $\mathbf{k}_\parallel$ and we find, with Eq. (16),

$$\langle T_j^{(2)}(k',k)\rangle \simeq -\delta_{\mathbf{k}'_\parallel,\mathbf{k}_\parallel}A/W_k\sum_{i=1}^{s}(k_{cj}^2 - k_{c,j-1}^2)(k_{ci}^2 - k_{c,i-1}^2)E_j(k')E_i(k)E_{j_>}(k)E_{j_<}(\bar{k})\sigma_{j_>}^2\tilde{c}_{ji}^{\perp}(0). \tag{20}$$

If the perpendicular correlation is also perfect $[\tilde{c}_{ji}^{\perp}(0)=1]$ and all the interfaces have the same roughness σ, the combined effect of first- and second-order contributions is, up to $O(k_0^2\sigma^2)$, that the total reflected field can be multiplied by a Debye-Waller (DW) factor $\exp(-2k_0^2\sigma^2)$. It can be shown that this is also true for large values of $k_0^2\sigma^2$ (Ref. 20) (cf. Appendix C).

Hence we have obtained expressions for both very small and very large correlation lengths and arbitrary roughness values, as well as for arbitrary correlation lengths and small roughness values. A problem is how to find a plausible interpolation. We obtained such an expression for one interface.[3] For multilayers such an interpolation is less obvious. If there is no correlation, the single-interface reflection and transmission coefficients have to be combined independently. Hence it is a good approach to multiply each of them by the appropriate NC factor to obtain a multilayer reflection coefficient r_k^{NC}. If both lateral correlation and perpendicular correlation are perfect, as outlined above, a single DW factor applies and the reflectivity can be written as follows: $\tilde{r}_k = r_k^{(0)}\exp[(r_k^{(1)} + r_k^{(2)})/r_k^{(0)}]$. Now we want to interpolate between these two in such a way that the expression suggested in Ref. 3 is obtained for a single interface. One possibility is

$$\tilde{r}_k = fr_k^{(0)}\exp[(r_k^{(1)} + r_k^{(2)})/r_k^{(0)}] + (1-f)r_k^{\mathrm{NC}}\exp(r_k^{(2)})/r_k^{(0)}), \tag{21}$$

where f describes the degree of correlation ($0 \leq f \leq 1$). A convenient choice for f is the ratio of $r_k^{(2)}$ to its value for perfect correlation. However, we feel that, when perpendicular correlation is absent, the first term in Eq. (21) will then easily be overestimated. Hence we multiplied this ratio by a factor $\Pi_{j=1}^{s}\tilde{c}_{j,j-1}^{\perp}(0)$ to obtain f. Still, we have to be aware that the method introduced in this *ad hoc* manner may fail for large values of $k_j\sigma_j$, especially if the exponents involved are larger than 1.

C. Glancing-incidence x-ray fluorescence

In a previous publication[1] we gave formulas for calculating glancing-incidence XRF (GIXRF) intensities from lay-

ered materials. We will now consider the role of interface roughness in detail. In Ref. 4 this has already been done for samples with a single rough surface. Here we will extend that treatment to samples with many rough interfaces.

In order to calculate the XRF intensities, we have to know the electric field inside the sample. In layer j this field is as given by Eq. (5). It is convenient to rewrite this expression as

$$\phi_{\mathbf{k}}^{(n)}(\mathbf{r})=\frac{A}{4\pi^2}\int d^2\mathbf{p}_{\parallel}\,\exp(i\mathbf{p}_{\parallel}\cdot\mathbf{x})[U_j^{\downarrow(n)}(p,k)\exp(ip_jz_j)+U_j^{\uparrow(n)}(p,k)\exp(-ip_jz_j)], \tag{22}$$

where

$$U_j^{\downarrow(n)}(p,k)=-\frac{1}{AW_k}\left[E_j^{\downarrow}(p)\sum_{i=1}^{j}T_i^{(n)}(\bar{p},k)+E_j^{\downarrow}(\bar{p})\sum_{i=j+1}^{s}T_i^{(n)}(p,k)\right],$$

$$U_j^{\uparrow(n)}(p,k)=-\frac{1}{AW_k}\left[E_j^{\uparrow}(p)\sum_{i=1}^{j}T_i^{(n)}(\bar{p},k)+E_j^{\uparrow}(\bar{p})\sum_{i=j+1}^{s}T_i^{(n)}(p,k)\right]. \tag{23}$$

The specular component of the field can be written as

$$\phi_{\mathbf{k},\mathrm{spec}}^{(n)}(\mathbf{r})=[\langle U_j^{\downarrow(n)}(k,k)\rangle\exp(ik_jz_j)+\langle U_j^{\uparrow(n)}(k,k)\rangle\exp(-ik_jz_j)]\exp(i\mathbf{k}_{\parallel}\cdot\mathbf{x}).$$

The intensity due to the incident x rays at position $\mathbf{r}$ is proportional to

$$|\phi_{\mathbf{k}}(\mathbf{r})|^2=|\phi_{\mathbf{k}}^{(0)}(\mathbf{r})|^2+2\,\mathrm{Re}[\phi_{\mathbf{k}}^{(0)*}(\mathbf{r})\phi_{\mathbf{k}}^{(1)}(\mathbf{r})+\phi_{\mathbf{k}}^{(0)*}(\mathbf{r})\phi_{\mathbf{k}}^{(2)}(\mathbf{r})+\cdots]+|\phi_{\mathbf{k}}^{(1)}(\mathbf{r})|^2+|\phi_{\mathbf{k}}^{(2)}(\mathbf{r})|^2+\cdots\,.$$

We will consider XRF from atoms which are distributed homogeneously across the considered layer j which has a thickness d_j. At a lateral position $\mathbf{x}$ the XRF intensity is proportional to

$$\int_{h_{j+1}(\mathbf{x})-d_j}^{h_j(\mathbf{x})}dz_j|\phi_{\mathbf{k}}(\mathbf{r})|^2\,\exp(\mu_jz_j),$$

where $h_j(\mathbf{x})$ and $h_{j+1}(\mathbf{x})$ are the height deviations of the ideal top and bottom interfaces, respectively, and μ_j is the linear absorption coefficient in layer j of the XRF radiation emitted perpendicular to the surface. Now we can split the integral into a term describing bulk absorption and two terms describing absorption in the interfacial layers:

$$\int_{h_{j+1}(\mathbf{x})-d_j}^{h_j(\mathbf{x})}dz_jf(z_j)=\int_{-d_j}^{0}dz_jf(z_j)+\int_{0}^{h_j(\mathbf{x})}dz_jf(z_j)-\int_{0}^{h_{j+1}(\mathbf{x})}dz_{j+1}f(z_{j+1}-d_j).$$

Below we will consider these terms separately. Furthermore, we have to integrate over $\mathbf{x}$ and to take a configurational average. We will normalize to unit surface area by dividing by A. The total intensity of the considered fluorescent line can be obtained from the following expressions by multiplying them by the amount of considered fluorescent atoms in layer j and the attenuation factor of the XRF radiation, $\exp(-\Sigma_{i=1}^{j-1}\mu_id_i)$, then summing over all the layers j in which the atoms are present, multiplying by the appropriate absorption coefficient, fluorescence yield, etc.

If we continue to the same order as in the previous subsection, we find that six contributions are important (I_0 to I_5):

(1) Absorption of the directly transmitted beam as though there were no roughness:

$$\begin{aligned}I_0&=A^{-1}\int d^2\mathbf{x}\int_{-d_j}^{0}dz_j|\phi_{\mathbf{k}}^{(0)}(\mathbf{r})|^2\,\exp(\mu_jz_j)\\&=|E_j^{\downarrow}(k)|^2\,\frac{1-\exp[-(2k_j''+\mu_j)d_j]}{2k_j''+\mu_j}+|E_j^{\uparrow}(k)|^2\,\frac{1-\exp[-(-2k_j''+\mu_j)d_j]}{-2k_j''+\mu_j}\\&\quad+2\,\mathrm{Re}\left\{E_j^{\downarrow}{}^*(k)E_j^{\uparrow}(k)\,\frac{1-\exp[-(2ik_j'+\mu_j)d_j]}{2ik_j'+\mu_j}\right\},\end{aligned}$$

where $k_j'=\mathrm{Re}(k_j)$ and $k_j''=-\mathrm{Im}(k_j)$.

(2), (3) The first- and second-order contributions, respectively, due to the change brought about in the transmitted intensity by the roughness:

$$2\,\mathrm{Re}\left\langle A^{-1}\int d^2\mathbf{x}\int_{-d_j}^{0} dz_j \phi_{\mathbf{k}}^{(0)*}(\mathbf{r})\phi_{\mathbf{k}}^{(n)}(\mathbf{r})\exp(\mu_j z_j)\right\rangle$$

$$=2\,\mathrm{Re}\left[\int_{-d_j}^{0} dz_j \phi_{\mathbf{k}}^{(0)*}(\mathbf{r})\phi_{\mathbf{k},\mathrm{spec}}^{(n)}(\mathbf{r})\exp(\mu_j z_j)\right]$$

$$=2\,\mathrm{Re}\Bigg\{E_j^{\downarrow *}(k)\langle U_j^{\downarrow(n)}(k,k)\rangle \frac{1-\exp[-(2k_j''+\mu_j)d_j]}{2k_j''+\mu_j} + E_j^{\uparrow *}(k)\langle U_j^{\uparrow(n)}(k,k)\rangle \frac{1-\exp[-(-2k_j''+\mu_j)d_j]}{-2k_j''+\mu_j} + [E_j^{\downarrow *}(k)\langle U_j^{\uparrow(n)}(k,k)\rangle + E_j^{\uparrow}(k)\langle U_j^{\downarrow(n)*}(k,k)\rangle]\frac{1-\exp[-(2ik_j'+\mu_j)d_j]}{2ik_j'+\mu_j}\Bigg\}.$$

For $n=1$, Eqs. (23) and (11) can be substituted to give I_1. An equivalent result is obtained when NC factors are used in the calculation of the fields in I_0. This implies that the reflection coefficients are multiplied by $\exp(-2k_{j-1}k_j\sigma_j^2)$ (cf. Sec. II B) and the transmission coefficients by $\exp[(k_j-k_{j-1})^2\sigma_j^2/2]$.[18] The intensity calculated in this way is equal to I_0+I_1 up to $O(k_j^2\sigma_j^2)$. For $n=2$, Eqs. (23) and (19) can be substituted to give I_2. If $k_0^2\xi_j/k\ll 1$, I_2 can be neglected; if $k_0^2\xi_j/k\gg 1$, Eq. (20) can be used.

We will use a procedure similar to that used for specular reflectivity in Sec. II B to extrapolate our results to the case of a greater degree of roughness. That is, if both ξ and $\xi_\perp$ are small, the NC result (for layer j) is multiplied by $\exp(I_2/I_0)$. For the perfectly correlated case, the zero-order fields have to be multiplied by the appropriate DW factors, which are $\exp[-(k_0-k_j)^2\sigma^2/2]$ for the downgoing field and $\exp[-(k_0+k_j)^2\sigma^2/2]$ for the upgoing field (see Appendix C). Equivalently, we can consider the three terms (due to downgoing x rays, upgoing x rays, and interference) in the intensity separately and multiply each zero-order term by the exponent of the first- and second-order terms summed, divided by the zero-order term.

(4) Absorption of diffusely scattered radiation:

$$I_3=\left\langle A^{-1}\int d^2\mathbf{x}\int_{-d_j}^{0} dz_j|\phi_{\mathbf{k}}^{(1)}(\mathbf{r})|^2\exp(\mu_j z_j)\right\rangle$$

$$=\frac{A}{4\pi^2}\int d^2\mathbf{p}_\parallel\Bigg\{\langle|U_j^{\downarrow(1)}(p,k)|^2\rangle\frac{1-\exp[-(2p_j''+\mu_j)d]}{2p_j''+\mu_j} + \langle|U_j^{\uparrow(1)}(p,k)|^2\rangle\frac{1-\exp[-(-2p_j''+\mu_j)d]}{-2p_j''+\mu_j} + 2\,\mathrm{Re}\left(\langle U_j^{\downarrow(1)*}(p,k)U_j^{\uparrow(1)}(p,k)\rangle\frac{1-\exp[-(2ip_j'+\mu_j)d]}{2ip_j'+\mu_j}\right)\Bigg\}.$$

In calculating configurational averages like $\langle|U_j^{\downarrow(1)}(p,k)|^2\rangle$, we have to evaluate averages of products of $T_i^{(1)}(p,k)$. As in the previous subsection, we have to integrate over $\mathbf{p}_\parallel$ and are not interested in the details of its shape. Hence we assume that we are allowed to use an expression similar to Eq. (18). With Eq. (23) we find

$$\langle|U_j^{\downarrow(1)}(p,k)|^2\rangle=\frac{1}{A|W_k|^2}\sum_{i=1}^{s}\sum_{i'=1}^{s}(k_{ci}^2-k_{c,i-1}^2)^*(k_{c,i'}^2-k_{c,i'-1}^2)\tilde{C}_{ii'}(\mathbf{p}_\parallel-\mathbf{k}_\parallel) \times E_i^*(k)E_{i'}(k)\begin{cases}|E_j^{\downarrow}(p)|^2E_i^*(\bar{p})E_{i'}(\bar{p}) & \text{if } i\leqslant j,\ i'\leqslant j,\\ |E_j^{\downarrow}(\bar{p})|^2E_i^*(p)E_{i'}(p) & \text{if } i>j,\ i'>j,\\ E_j^{\downarrow *}(p)E_j^{\downarrow}(\bar{p})E_i^*(\bar{p})E_{i'}(p) & \text{if } i\leqslant j,\ i'>j,\\ E_j^{\downarrow *}(\bar{p})E_j^{\downarrow}(p)E_i^*(p)E_{i'}(\bar{p}) & \text{if } i>j,\ i'\leqslant j,\end{cases}$$

and analogous expressions for $\langle|U_j^{\uparrow(1)}(p,k)|^2\rangle$ and $\langle U_j^{\downarrow(1)*}(p,k)U_j^{\uparrow(1)}(p,k)\rangle$. If $k_0^2\xi_j/k\ll 1$, I_3 may be neglected; if $k_0^2\xi_j/k\gg 1$, we can substitute Eq. (16) with $\tilde{C}_j(\mathbf{q}_\parallel)\simeq 4\pi^2\sigma_j^2\delta(\mathbf{q}_\parallel)$ in the above expressions.

(5) Absorption of the direct beam in the rough interfacial layers. At the top interface (j),

$$I_{4,1}=\left\langle A^{-1}\int d^2\mathbf{x}\int_0^{h_j(\mathbf{x})} dz_j|\phi_{\mathbf{k}}^{(0)}(\mathbf{r})|^2 \exp(\mu_j z_j)\right\rangle$$

$$=\left\langle A^{-1}\int d^2\mathbf{x}\left(|E_j^{\downarrow}(k)|^2 \frac{\exp[(2k_j''+\mu_j)h_j(\mathbf{x})]-1}{2k_j''+\mu_j} + |E_j^{\uparrow}(k)|^2 \frac{\exp[(-2k_j''+\mu_j)h_j(\mathbf{x})]-1}{-2k_j''+\mu_j} + 2\,\mathrm{Re}\left\{ E_j^{\downarrow *}(k)E_j^{\uparrow}(k)\frac{\exp[(2ik_j'+\mu_j)h_j(\mathbf{x})]-1}{2ik_j'+\mu_j}\right\}\right)\right\rangle$$

$$=|E_j^{\downarrow}(k)|^2 \frac{\exp[(2k_j''+\mu_j)^2\sigma_j^2/2]-1}{2k_j''+\mu_j} + |E_j^{\uparrow}(k)|^2 \frac{\exp[(-2k_j''+\mu_j)^2\sigma_j^2/2]-1}{-2k_j''+\mu_j} + 2\,\mathrm{Re}\left\{ E_j^{\downarrow *}(k)E_j^{\uparrow}(k)\frac{\exp[(2ik_j'+\mu_j)^2\sigma_j^2/2]-1}{2ik_j'+\mu_j}\right\}.$$

Absorption by the considered fluorescent atoms of layer j at the bottom interface $(j+1)$:

$$I_{4,2}=-\exp(-\mu_j d_j)\left\langle A^{-1}\int d^2\mathbf{x}\int_0^{h_{j+1}(\mathbf{x})} dz_{j+1}|\phi_{\mathbf{k}}^{(0)}(\mathbf{r})|^2 \exp(\mu_j z_{j+1})\right\rangle$$

$$=-\exp(-\mu_j d_j)\left(|E_{j+1}^{\downarrow}(k)|^2 \frac{\exp[(2k_{j+1}''+\mu_j)^2\sigma_{j+1}^2/2]-1}{2k_{j+1}''+\mu_j} + |E_{j+1}^{\uparrow}(k)|^2 \frac{\exp[(-2k_{j+1}''+\mu_j)^2\sigma_{j+1}^2/2]-1}{-2k_{j+1}''+\mu_j} + 2\,\mathrm{Re}\left\{ E_{j+1}^{\downarrow *}(k)E_{j+1}^{\uparrow}(k)\frac{\exp[(2ik_{j+1}'+\mu_j)^2\sigma_{j+1}^2/2]-1}{2ik_{j+1}'+\mu_j}\right\}\right).$$

(6) Correction to (5) due to the change in the intensity caused by the roughness. At the top interface j,

$$I_{5,1}=2\,\mathrm{Re}\left\langle A^{-1}\int d^2\mathbf{x}\int_0^{h_j(\mathbf{x})} dz_j\phi_{\mathbf{k}}^{(0)*}(\mathbf{r})\phi_{\mathbf{k}}^{(1)}(\mathbf{r})\exp(\mu_j z_j)\right\rangle$$

$$\simeq 2\,\mathrm{Re}\left\langle \frac{1}{4\pi^2}\int d^2\mathbf{p}_{\parallel}\int d^2\mathbf{x}\,\exp[i(\mathbf{p}_{\parallel}-\mathbf{k}_{\parallel})\cdot\mathbf{x}][E_j^{\downarrow}(k)+E_j^{\uparrow}(k)]^*[U_j^{\downarrow(1)}(p,k)+U_j^{\uparrow(1)}(p,k)]h_j(\mathbf{x})\right\rangle.$$

Again, we only continue to second order in $k_j h_j(\mathbf{x})$. That implies that $U_j^{\downarrow(1)}(p,k)$ and $U_j^{\uparrow(1)}(p,k)$ only have to be evaluated up to the first order in $k_j h_j(\mathbf{x})$. Then Eq. (10) can be written as

$$T_j^{(1)}(p,k)\simeq(k_{cj}^2-k_{c,j-1}^2)E_j(p)E_j(k)\int d^2\mathbf{x}\,\exp[i(\mathbf{p}_{\parallel}-\mathbf{k}_{\parallel})\cdot\mathbf{x}]h_j(\mathbf{x}).$$

This leads to the product of $h_j(\mathbf{x})$ and $h_i(\mathbf{x})$ in $I_{5,1}$. The configurational average results in the correlation function $C_{ji}(\mathbf{x})$. We obtain

$$I_{5,1}\simeq 2\,\mathrm{Re}\left\{-\frac{1}{4\pi^2 W_k}E_j^*(k)\int d^2\mathbf{p}_{\parallel}\sum_{i=1}^{s}(k_{ci}^2-k_{c,i-1}^2)\tilde{C}_{ji}(\mathbf{p}_{\parallel}-\mathbf{k}_{\parallel})E_{j_>}(p)E_{j_<}(\bar{p})E_i(k)\right\}.$$

At the bottom interface $(j+1)$,

$$I_{5,2}=2\,\mathrm{Re}\left\langle -\exp(-\mu_j d_j)A^{-1}\int d^2\mathbf{x}\int_0^{h_{j+1}(\mathbf{x})} dz_{j+1}\phi_{\mathbf{k}}^{(0)*}(\mathbf{r})\phi_{\mathbf{k}}^{(1)}(\mathbf{r})\exp(\mu_j z_{j+1})\right\rangle$$

$$\simeq 2\,\mathrm{Re}\left\{\frac{1}{4\pi^2 W_k}\exp(-\mu_j d_j)E_{j+1}^*(k)\int d^2\mathbf{p}_{\parallel}\sum_{i=1}^{s}(k_{ci}^2-k_{c,i-1}^2)\tilde{C}_{j+1,i}(\mathbf{p}_{\parallel}-\mathbf{k}_{\parallel})E_{i_{1_>}}(p)E_{i_{1_<}}(\bar{p})E_i(k)\right\},$$

where $i_{1_>} \equiv \max(j+1,i)$ and $i_{1_<} \equiv \min(j+1,i)$. As for I_2 and I_3, if $k_0^2\xi_j/k \ll 1$, I_5 may be neglected, and if $k_0^2\xi_j/k \gg 1$, we can substitute $\tilde{C}_j(\mathbf{q}_\parallel) \simeq 4\pi^2\sigma_j^2\delta(\mathbf{q}_\parallel)$.

Other contributions will not be taken into account, since they are smaller by at least a factor of $O(k_0^2\sigma_j^2)$ (cf. Appendix B). We note that, for small values of ξ_j, only corrections (2) and (5) apply. In existing algorithms[1] only correction (2) is used. This is not completely correct since, as will be seen below, contribution (5) may also have an appreciable influence.

III. GRADED INTERFACES AS A STARTING POINT

A better starting point for the DWBA than that corresponding to flat interfaces may be that corresponding to graded interfaces resulting from a lateral averaging of the refractive index.[7] This will be the case unless the lateral correlation length of the roughness is very large ($\xi k_0^2/|\mathbf{k}| \gg 1$: cf. Ref. 4). The lateral width over which averaging has to take place is equal to the coherence length of the x rays, which is $2\pi/(k_0\Delta\theta)$, where $\Delta\theta$ is the divergence of the incident x rays.

For a Gaussian distribution of interface heights, the refractive-index profile is an error function. In that case the Helmholtz equation (1) cannot be exactly solved. We will not use a profile that can be solved exactly instead (like a tangent hyperbolicus[7,21,22]), but will look for a suitable approximation.

Hence we will consider $V_0(z)$ to be an error function around each average interface position, whereas $V_1(\mathbf{r})$ represents the actual jump in refractive index minus $V_0(z)$. We will assume that the unperturbed solution of Eq. (1) can be written in a form analogous to Eq. (3), but with depth-dependent amplitudes and wave vectors. Then the perturbed fields will have a form analogous to Eq. (5), the T matrix being calculated using these unperturbed fields. The first-order specular contribution to the T matrix will consist of a term containing the average of the integral of the refractive index minus a term containing the integral of the average of the refractive index. This contribution vanishes.

To be able to calculate the higher-order contributions, we have to incorporate the right depth dependence of amplitudes and wave vectors. We will make the simplifying assumption that in the graded region around interface j the electric field can be written as

$$\psi_k(z_j) = E_g^{\downarrow}(k)\exp(ik_g z_j) + E_g^{\uparrow}(k)\exp(-ik_g z_j); \quad (24)$$

i.e., we suppose that in good approximation one effective wave vector and one set of amplitudes can be used for the interfacial region. Then the diffuse-scattering cross section, for instance, can be written in a form very similar to Eq. (14), with the interfacial amplitudes and wave vectors being substituted by $E_g^{\downarrow}(k)$, $E_g^{\uparrow}(k)$, and k_g.

Before we discuss the consequences of this approach in more detail, we will try to find a good approximation for calculating Eq. (24) for the case of graded interfaces. One possible approach is to take the self-consistent fields which contain the reflection and transmission coefficients multiplied by the appropriate NC factors. In Secs. II B and II C, we mentioned that this is a good approximation for calculating reflectivity and GIXRF for rough interfaces with Gaussian height distributions. If the fields obtained in this way

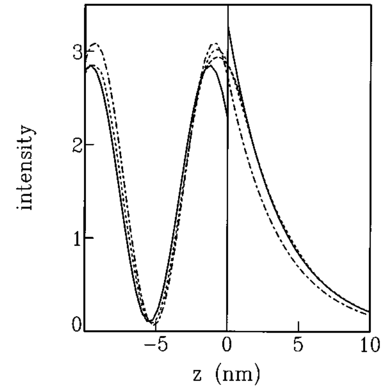

FIG. 2. X-ray intensity vs depth for Cu $K\alpha$ radiation with a perpendicular wave vector $k_0 = 0.375\ \mathrm{nm}^{-1}$ on a gold sample with a rms roughness of 1.5 nm. Dash-dotted line, no roughness; solid line, calculated using NC factors; long-dashed line, approximation (see text); short-dashed line, calculated for error-function profile using slice method.

were to be good approximations to the real fields, the diffuse-scattering cross section would be given by Eq. (14) with the amplitudes calculated for the rough interfaces. This suggestion was made for a single interface by Weber and Lengeler,[23] and a similar approach was followed by Kopecky.[24] However, as mentioned above, the electric fields obtained in this way are only correct for small values of $k_j^2\sigma_j^2$ and/or small small values of $(k_{cj}^2 - k_{c,j-1}^2)/k_j^2$. (The reason for this is that, in deriving the NC formulas, the fields are approximated by the expressions strictly valid at one side of the interface only.[19,21])

In Fig. 2 we see that serious errors may indeed be made. In this figure the intensity due to the incident x rays is drawn in the neighborhood of a rough air-gold interface at an incidence angle close to the critical angle. Note that here neither $k_j^2\sigma_j^2$ nor $(k_{cj}^2 - k_{c,j-1}^2)/k_j^2$ is small. Above the interface there is an x-ray standing wave due to interference of the incident and reflected beams and below the interface an evanescent wave. The numerical solution obtained via the slice method mentioned above (short dashes) and the solution obtained with the aid of NC factors (solid line) are both indicated. Away from the interface both solutions coincide surprisingly well. (The phase of the reflected wave is slightly different: cf. Ref. 21.) This indicates that it is correct to calculate the reflectivity and transmissivity by using NC factors. In the neighborhood of the interface, however, the two differ. The approximate solution has a discontinuity at the interface, whereas the real solution varies smoothly. It can be seen that close to the interface the field for a flat interface is a better approximation than that obtained using NC factors. This is in agreement with the findings of Holý,[25] who did a scattering calculation using the numerical solutions as a starting point.

Another approach is to solve Eq. (1) numerically by dividing the error-function profile into many very thin slices in which the refractive index may be considered constant. Then the fields can be found using standard methods.[10,11] As we will see below, these fields can be used directly to calculate the GIXRF intensities for the case of small lateral correlation. It is not feasible to use these fields directly for calcu-

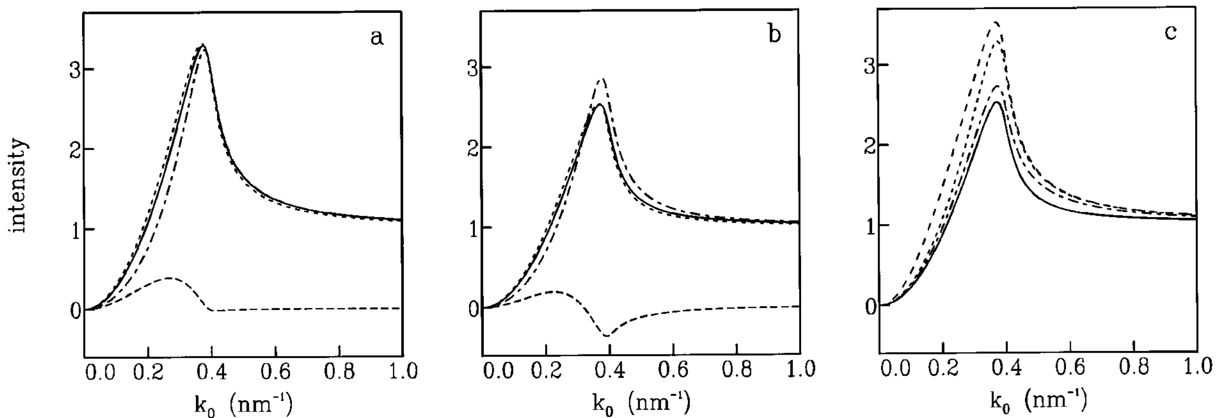

FIG. 3. Calculated GIXRF intensities vs perpendicular incident wave vector k_0 for Cu $K\alpha$ radiation incident on a gold sample with a rms roughness of 1.5 nm. All the intensities have been normalized to unity at a high angle. (a) Au bulk intensity (multiplied by k''_{Au}). Dash-dotted line, bulk absorption (I_0+I_1); long dashes, correction due to absorption in rough interfacial layer (I_4); solid line, total intensity; short dashes, calculated using error-function graded interface. (b) Intensity for a submonolayer surface layer. Dash-dotted line, absorption if the layer were flat (I_0+I_1); long dashes, correction due to absorption in rough interfacial layers (I_4); solid line, total intensity; short dashes, calculated using error-function graded interface. (c) Dash-dotted line, no roughness; long dashes, calculated using flat interfaces as a starting point; short dashes, calculated using the method for bulk [cf. (a)]; solid line, calculated using the method for the surface layer [cf. (b)].

lating diffuse scattering. One possibility is to use the fields found for the middle of the graded region, but these fields will not be correct at the borders of the graded region. (The same holds for the calculation of $r_k^{(2)}$, I_2, I_3, and I_5.)

We can try to make a better approximation by assuming that the fields obtained using the NC factors are correct except in an interfacial region.[26] Inside this region we calculate the wave vector k_g using the average of the refractive indices of the neighboring layers (which is correct at the average interface position). Then the amplitudes $E_g^{\downarrow}(k)$ and $E_g^{\uparrow}(k)$ can be calculated by assuming that the electric fields are continuous at the two boundaries. (The derivatives are not continuous.) The intensity obtained in this way has also been plotted in Fig. 2 (long dashes). It seems to be a reasonable approximation to that obtained using the slice method (short dashes).

We will now consider the consequences of this method for GIXRF in the case of small correlation lengths, i.e., for I_0, I_1, and I_4 of Sec. II C. Outside the interfacial regions we can use the NC factors to calculate the fields to obtain I_0. From the above discussion it follows that the first-order contribution I_1 vanishes. Hence I_0+I_1 remains essentially the same. The correction due to absorption in the rough interfacial layers (I_4) will differ, however, since it involves the fields close to the interface. We will use the amplitudes and wave vectors obtained using the new method to calculate I_4.

As an example, we will discuss the results obtained for a rough gold sample, i.e., the same case as that of Fig. 2. In Fig. 3 we compare the GIXRF intensities as a function of the perpendicular incident wave vector k_0, calculated in different approximations. In Fig. 3 of Ref. 4, we already gave the result of calculations when flat interfaces are used as a starting point for the DWBA [reproduced as the long-dashed line in Fig. 3(c)]. Here we show the results for two cases: a gold bulk sample and a submonolayer of impurities at the interface. In the bulk case [Fig. 3(a)], the intensity has been multiplied by the imaginary part of the wave vector (while μ_{Au} has been neglected). Qualitatively, the results are similar to those of Ref. 4, but both cases only yield the same result [dash-dotted line in Fig. 3(c)] if there is no roughness. Different results are obtained for the rough samples: Fig. 3(a) for gold bulk and Fig. 3(b) for the submonolayer at the interface, also shown as the short-dashed and solid curve of Fig. 3(c), respectively. Note that the contribution due to absorption in the rough interfacial layers [long dashes in Figs. 3(a) and 3(b)] is appreciable. The reason why the total intensity is lower for the submonolayer case is that a large part of the interface lies deeper with respect to the average interface, where the x-ray intensity is lower (cf. Fig. 2). We also did calculations using the slice method for the error-function profile [short-dashed lines in Figs. 3(a) and 3(b)]. It can be seen that the agreement with the results obtained using the approximate method (solid lines) is very good. We consequently also consider the approximate method a reliable method for calculating diffuse scattering and $r_k^{(2)}$.

As an example of diffuse scattering calculations, we compare in Fig. 4 intensities obtained for a single interface using the various approximations.[27] The example, a transverse (or rocking) scan on a rough aluminum sample, is the same as that given by Weber and Lengeler.[23] They fitted their experimental data using the fields calculated with the aid of NC factors. The intensities calculated with this method, shown as the solid lines in Fig. 4, fit their data well. We compare these with those calculated using the unperturbed fields [dashed line in Fig. 4(a)] and those obtained using our method (i.e., using the approximate fields for the interfacial region, dashed line in Fig. 4(b)]. There are significant differences between the three. Moreover, with somewhat different parameters it is possible to obtain intensities very similar to the original data [dot-dashed lines in Figs. 4(a) and 4(b)], using both the unperturbed fields[28] and the perturbed fields.

We have to note that this approach to diffuse scattering is only valid in the case of small correlation lengths ($\xi k_0^2/|\mathbf{k}|<1$, a condition which is only just fulfilled in the above case). In Ref. 4 we obtained formulas for the scattering at a single interface in the case of large correlation

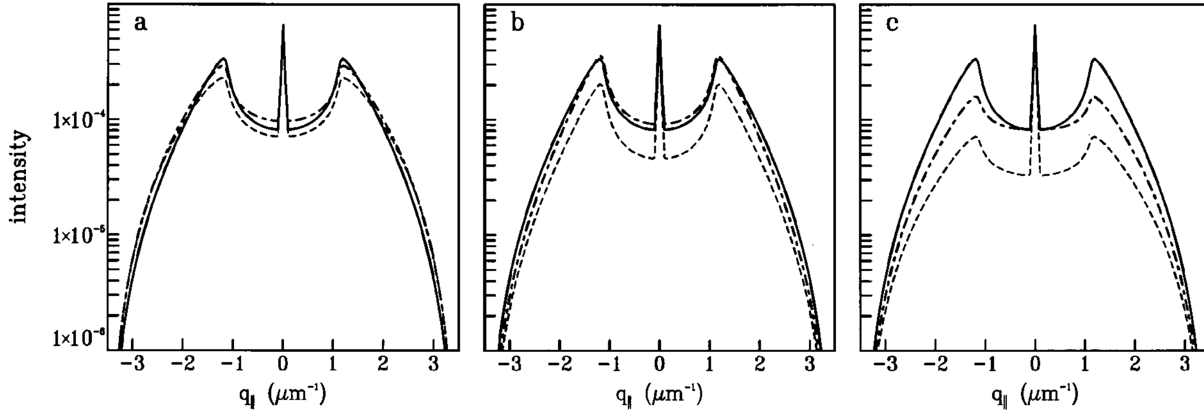

FIG. 4. Calculated scattered intensity vs parallel wave-vector transfer in a transverse scan at $k_0+p_0=0.495\ \mathrm{nm}^{-1}$ for scattering of x rays with a wavelength of 0.177 nm on an aluminum sample with a rms roughness of 4 nm. In all three figures the solid line was obtained using NC factors, a correlation length $\xi=400$ nm and $H=1$. (a) Dashed line, calculated using unperturbed fields $\xi=400$ nm and $H=1$. Dot-dashed line, calculated using unperturbed fields, $\xi=600$ nm, and $H=0.7$. (b) Dashed line, calculated using graded interfaces as a starting point, $\xi=400$ nm and $H=1$. Dot-dashed line, calculated using graded interfaces as a starting point, $\xi=800$ nm and $H=1$. (c) Dashed line, calculated using the method for large correlation lengths, $\xi=400$ nm and $H=1$. Dot-dashed line, calculated using the method for large correlation lengths, $\xi=1000$ nm and $H=1$.

lengths. (Unfortunately, such a formalism is not yet known for layered materials, for which one has to take into account the correlation between the various interfaces, as explained in the discussion in Sec. II B.) In Fig. 4(c) we show the results obtained using this approach (dashed line). We were unable to fit the original data in this model [cf. dot-dashed line in Fig. 4(c)]. This indicates that the correlation length is too small for this model to be applicable.

Next we will consider how we can deal with specular reflectivity using the method. As in the case of GIXRF, the zero-order contribution is essentially that obtained using NC factors, whereas the first-order contribution vanishes. Hence $r_k^{(0)}+r_k^{(1)}$ remains the same. Since the DW result should be obtained in the case of perfect correlation, we will use the unperturbed fields to obtain the first term of Eq. (21). For the second term, however, we will use the fields obtained using the method presented here.[29] (Although this approach differs somewhat from that of Ref. 3, we found that the differences for a single interface can be neglected.)

This same procedure will be followed to obtain the contribution I_2 to the GIXRF intensities. For the contributions I_3 and I_5, we will use the fields obtained using graded interfaces, unless $\xi k_0^2/|\mathbf{k}|\gg 1$. Below we will give some examples of the calculation of reflectivity and GIXRF for samples with more than one rough interface.

IV. EXAMPLES OF CALCULATIONS FOR LAYERED MATERIALS

First we will show calculations for a single layer of 30 nm silicon on a gold substrate. In that case waveguidelike behavior may occur just above the critical angle for silicon,[1] yielding a dip in the reflectivity at approximately $0.18\ \mathrm{nm}^{-1}$. Figure 5 shows the reflectivity for various values of the rms roughness and correlation lengths. In Fig. 5(a) both interfaces have the same roughness, in Figs. 5(b) and 5(c) the interfaces have different roughnesses. When the case without roughness (long dashes in all three figures) is compared with the cases with roughness but without correlation (solid lines), it can be seen that the effect of the NC factor may be to

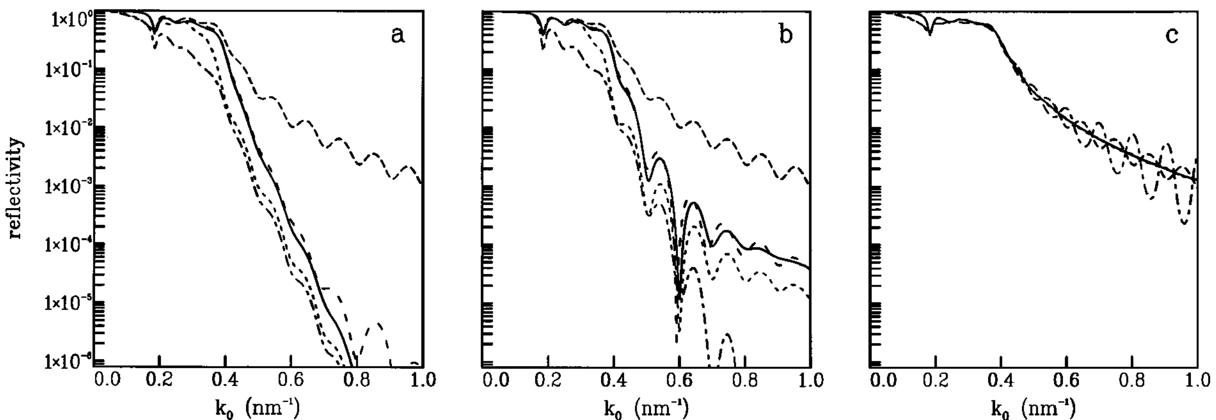

FIG. 5. Calculated reflectivity for Cu $K\alpha$ incident on a sample consisting of 30 nm Si on Au with different interface roughnesses: (a) $\sigma_{\mathrm{air/Si}}=2$ nm, $\sigma_{\mathrm{Si/Au}}=2$ nm. (b) $\sigma_{\mathrm{air/Si}}=0$ nm, $\sigma_{\mathrm{Si/Au}}=2$ nm. (c) $\sigma_{\mathrm{air/Si}}=2$ nm, $\sigma_{\mathrm{Si/Au}}=0$ nm. Long dashes (upper curve), no roughness; solid line, $\xi=0$, $\xi_\perp=0$; widely spaced dashes, error-function profiles; short dashes, $\xi=\infty$, $\xi_\perp=0$; dot-dashed line, $\xi=\infty$, $\xi_\perp=\infty$.

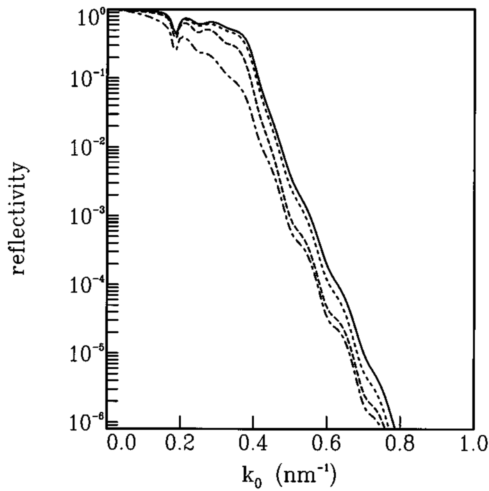

FIG. 6. Influence of lateral correlation length ξ on reflectivity calculated for Cu $K\alpha$ incident on the sample of Fig. 5(a) with $\xi_\perp=\infty$. Solid line, $\xi=0$; short dashes, $\xi=100$ nm; long dashes, $\xi=1000$ nm; dot-dashed line, $\xi=\infty$.

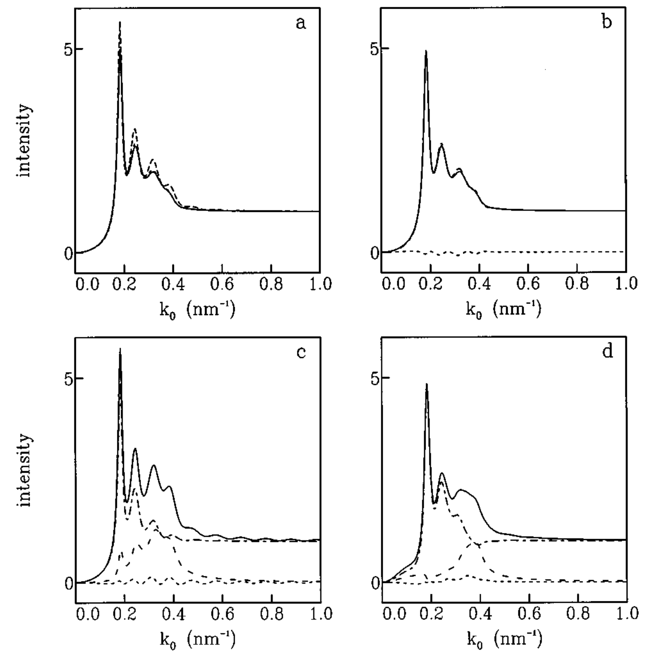

FIG. 7. Si $K\alpha$ GIXRF (excited by Cu $K\alpha$) calculated for a sample consisting of 30 nm Si on Au with $\sigma_{air/Si}=2$ nm, $\sigma_{Si/Au}=2$ nm [cf. Fig. 5(a)]. (a) and (b) $\xi=0$, $\xi_\perp=0$; (c) $\xi=\infty$, $\xi_\perp=\infty$; (d) $\xi=\infty$, $\xi_\perp=0$. For (a), long dashes, I_0 ($\sigma_{air/Si}=\sigma_{Si/Au}=0$); small dashes, calculated using error-function profile; solid line, total intensity for rough interfaces [see (b)]. For (b), dot-dashed line, absorption of directly transmitted radiation (I_0+I_1); short dashes, absorption in rough interfaces (I_4); solid line, total intensity. For (c) and (d), dot-dashed line, absorption of directly transmitted radiation $(I_0+I_1+I_2)$; long dashes, absorption of diffusely scattered radiation (I_3); short dashes, absorption in rough interfaces (I_4+I_5); solid line, total intensity.

reduce the overall reflectivity and/or to affect the fringe amplitude. In general, there is good agreement with the error-function profile (widely spaced dashes), although at large values of k_0 the slicing method may cause false oscillations [Fig. 5(a)]. (The manner of slicing affects this behavior.) In the case that lateral and perpendicular correlations are both perfect, the DW factor can be used and the reflectivity is reduced even more than in the NC case [Fig. 5(a), dot-dashed line]. As for single interfaces,[3] the difference between the two is maximum at the critical angle and goes to a constant factor at large angles of incidence. In Figs. 5(b) and 5(c) the case of perfect correlation (dot-dashed lines) is unphysical, since the roughnesses of the two interfaces are different. However, we may see what the trend of the effect of correlation is. In Fig. 5(b) a reduction of the reflectivity can again be seen. In Fig. 5(c) the result is a reduction of fringe maxima and an enhancement of fringe minima. We believe that the reversion of the order of maxima and minima is an artifact of the calculation. If there is no perpendicular correlation (short dashes), the reflectivity is somewhere in between.

Next we will consider the effect of a finite lateral correlation length. In Fig. 6 we show the results of calculations for the sample of Fig. 5(a). We chose the same value ξ for the correlation lengths of the two interfaces and assumed the correlation between the two interfaces to be perfect. We see a gradual change between the NC and DW cases, as also obtained for a single interface.[3] We also performed calculations for the same sample without perpendicular correlation. Here we found that at $\xi\lesssim1000$ nm the results were hardly distinguishable from those obtained for perfect correlation, but at very large values of ξ the same results as shown in Fig. 5(a) were obtained.

Figure 7 shows the results of calculations of the Si GIXRF intensity (normalized at the high-angle value) for the sample of Fig. 5(a), again with various degrees of correlation. The large amplitude of the oscillations is due to waveguidelike behavior.[1] When compared with the case without roughness [Fig. 5(a), long dashes], the general effect of interface roughness is a reduction of the amplitude of the GIXRF fringes. Again, there is good agreement between the results obtained using the NC [Fig. 7(a), solid line] and the error-function method [Fig. 7(a), short dashes]. The absorption of the diffusely scattered radiation is appreciable in Figs. 7(c) and 7(d) (long dashes), where both the rms roughness and the lateral correlation length of the silicon-gold interface are large. The correction due to absorption in the rough interfacial layers (short dashes) is small in all cases. To account for the effect of roughness, we used the theory with graded interfaces as a starting point. We found that the results obtained using flat interfaces as a starting point are approximately the same.

The same kind of calculations can be performed for periodic multilayers. As an example, Fig. 8 shows the reflectivity for a tungsten-carbon multilayer with the first Bragg peak at approximately 1.1 nm^{-1}. Again, there is a good agreement between the results of calculations using the NC method and those performed using error-function profiles. Since the difference is negligible, both are indicated by the solid line in Fig. 8(a). The effect of the lateral correlation length [Fig. 8(c)] is small. Only in the Bragg peak do we see a decrease in intensity with an increasing correlation length. A decrease in the perpendicular correlation length leads to an increase in the Bragg peak intensity [Fig. 8(b)]. Unfortunately, we found that unphysically large intensities may be obtained when the

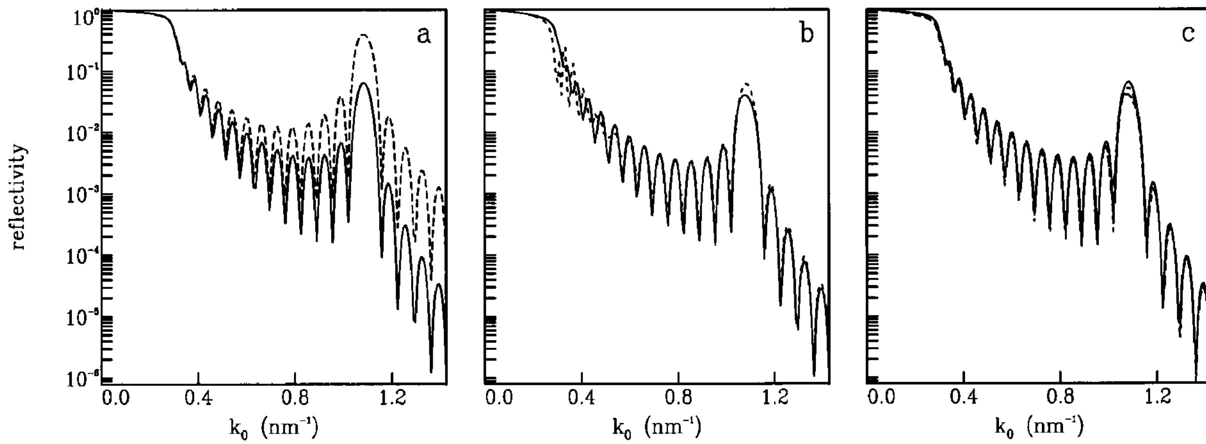

FIG. 8. Reflectivity calculated for Cu $K\alpha$ from samples consisting of 15 periods of 1.5 nm W and 1.5 nm C on a silicon substrate. We assumed σ=0.7 nm for all interfaces unless otherwise indicated. (a) Long dashes, no roughness; solid line, ξ=0, $\xi_\perp$=0. (b) Short dashes, $\xi=\infty$, $\xi_\perp$=0; solid line, $\xi=\infty$, $\xi_\perp=\infty$. (c) $\xi_\perp=\infty$ and various values of the lateral correlation length. Solid line, ξ=0 for all interfaces; dot-dashed line, ξ=300 nm for all interfaces; dashed line, $\xi=\infty$ for all interfaces.

perpendicular correlation is not perfect, since the second-order term of Eq. (21) may become very large. This is the cause of the false oscillations in the neighborhood of the critical angle in Fig. 8(b) (short dashes).

Figure 9 shows the W GIXRF intensities obtained for the same multilayer. Figures 9(a) and 9(b) are for the case with negligible correlation, showing the effect of what is used as starting point of the calculation. Figures 9(c) and 9(d) deal with the influence of correlation. In all cases a modulation near the Bragg peak is seen, caused by the x-ray standing wave formed due to interference between the incoming and reflected beams (cf. Ref. 1 and references therein). The antinodes of the x-ray standing wave are in the low-density (carbon) layers at the low-angle side and in the high-density (tungsten) layers at the low-angle side of the Bragg peak. In Figs. 9(a) and 9(b) the case of a small correlation length is dealt with in two approximations: using flat interfaces as a starting point [Fig. 9(a)] and using graded interfaces as a starting point [Fig. 9(b)]. When we compare the results with those obtained in the case without roughness [Fig. 9(a), long dashes], we see that roughness with small correlation lengths has two effects: The modulation of the transmission (I_0+I_1, dot-dashed line) is reduced, and the absorption in the rough interfaces (I_4, short dashes) is appreciable and has the opposite phase of modulation. The total intensity is shown as solid lines. When flat interfaces are taken as a starting point [Fig. 9(a)], the effect of the absorption in the rough interfaces is so great that the modulation changes sign. This result is unphysical, since it would indicate a reversal of the densities of tungsten and carbon. When graded interfaces are taken as a starting point [Fig. 9(b)], the effect is that there is hardly any modulation left. This is the expected effect, since the interface roughness is almost as large as the layer thicknesses. The agreement with the results of a calculation using error-function profiles [long dashes in Fig. 9(b)] is very good. This is a clear example of the method of Sec. III yielding results which are physically more acceptable than those obtained using flat interfaces as a starting point. For perfectly correlated interfaces [Fig. 9(c)], the correction for absorption in the rough interfaces (I_4+I_5, short dashes) has a sign opposite to that for noncorrelated interfaces. The transmission ($I_0+I_1+I_2$, dot-dashed line) has a dip which largely cancels the absorption of the diffusely scattered radiation (I_3, long dashes). The behavior of the total intensity (solid line) is qualitatively similar to that observed for layers without any roughness. For the case of no perpendicular correlation and $\xi=\infty$ [Fig. 9(d)], we find unphysical results in the neighborhood of the critical angle, as in Fig. 8(b). At the Bragg peak the result is similar to that obtained for small values of ξ [Fig. 9(b)].

V. CONCLUSIONS

A rough interface often can be considered as self-affine; that is, it can be characterized by three parameters: its rms roughness, its lateral correlation length, and its jaggedness parameter. For a multilayer at least one additional parameter is required, e.g., the perpendicular correlation length. We have presented a theory enabling the calculation of specular and diffuse reflectivity and GIXRF expressed in these parameters. Together with the results discussed in previous publications,[3,4] this leads to the following picture.

In the case of small lateral correlation lengths ($k_0^2\xi_j/|\mathbf{k}|\ll 1$), diffuse scattering may be neglected with respect to the specular reflectivity and a possible approach is to use the slicing method for graded interfaces. Alternatively, the reflection and transmission coefficients can be obtained in a self-consistent way, which results in NC factors.[17,21] However, in the latter case the fields close to the interfaces are not calculated correctly (see Fig. 2). Especially in cases of appreciable roughness and close to the critical wave vector or to Bragg peaks, the effect may be substantial.

In cases of greater lateral correlation lengths, in which diffuse scattering may not be neglected, the DWBA can be successfully applied. When the lateral correlation lengths are large ($k_0^2\xi_j/|\mathbf{k}|\gg 1$) and the rms roughness is appreciable, however, the DWBA for the calculation of diffuse scattering may break down, especially in the total-reflection region. In that case the Rayleigh approximation yields the correct behavior for single interfaces.[4] Such an approach is not (yet) available to calculate diffuse scattering for multilayers. The approach described in Appendix C for the specular case is,

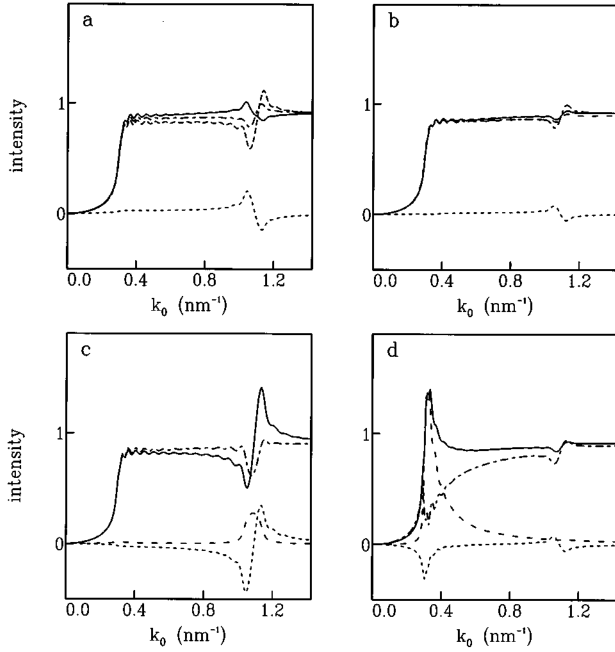

FIG. 9. W $M\alpha$ GIXRF (excited by Cu $K\alpha$) calculated for samples consisting of 15 periods of 1.5 nm W and 1.5 nm C on a silicon substrate. We assumed σ=0.7 nm for all interfaces unless otherwise indicated. (a) ξ=0, $\xi_\perp$=0, flat interfaces as a starting point; (b) ξ=0, $\xi_\perp$=0, graded interfaces as a starting point; (c) $\xi=\infty$, $\xi_\perp=\infty$; (d) $\xi=\infty$, $\xi_\perp$=0. For (a), long dashes, I_0 (no roughness); dot-dashed line, I_0+I_1 (absorption of direct transmitted radiation); small dashes, I_4 (absorption in rough interfaces); solid line, total intensity. For (b), dot-dashed line, I_0+I_1 (absorption of directly transmitted radiation); short dashes, I_4 (absorption in rough interfaces); solid line, total intensity; large dashes, error-function profile. For (c) and (d), dot-dashed line, $I_0+I_1+I_2$ (absorption of directly transmitted radiation); long dashes, I_3 (absorption of diffusely scattered radiation); short dashes, I_4+I_5 (absorption in rough interfaces); solid line, total intensity.

however, similar to the Rayleigh approximation. Far from total reflection and Bragg peaks, the simple Born approximation may suffice to give a good description of diffuse-scattering data.[12]

A point which we were able to settle in this paper is which fields to use as a starting point for the DWBA. If the rms roughness and reflectivity are both appreciable, one should use the solutions for the graded interface, as is clearly shown by the GIXRF examples [Figs. 3 and 9(a), 9(b)]. Since the fields obtained by using NC factors are not correct close to the interfaces, we have suggested a simple interpolation method for obtaining approximate fields which can be used as a starting point for the DWBA. The results obtained for GIXRF are very good.

For diffuse scattering the effect of this method is that the fields to be substituted are smaller, which results in intensities which are smaller by approximately a factor of 2 [see Fig. 4(b)].

We also investigated the effect of second-order terms in the DWBA. For diffuse scattering this effect is negligible, except in the case of substantial reflectivity, when the lateral correlation length and rms roughness are both large (Appendix B). This is in accordance with the aforementioned breakdown of the (first-order) DWBA.

For specular reflectivity and GIXRF, the first- and second-order perturbation terms are both of second order in the rms roughness. Only in the case of small lateral correlation lengths ($k_0^2\xi_j/|\mathbf{k}|\ll 1$) may the second-order contribution be neglected. A problem is that, strictly speaking, the DWBA is only valid for small roughness values ($k_0\sigma_j<1$) or far above the critical wave vector. We found a plausible way of extrapolating the results in the case of single interfaces.[3] For layered materials we found a reasonable description for the case of considerable correlation [cf. Figs. 6 and 8(c)]. If the perpendicular correlation is small, however, the DWBA may yield incorrect results for appreciable rms roughness values close to the critical wave vector [Figs. 8(b) and 9(d)].

In the case of GIXRF, there are several terms contributing up to second order (Sec. II C). A term which is also present for small correlation lengths, but which has so far been neglected,[1] is the absorption in the rough interfacial layers (I_4). This term is appreciable when both the rms roughness and the absorption coefficient are not too small. In the case of silicon (Fig. 7), this has hardly any effect, but in the case of heavy materials like gold or tungsten it may not be neglected (Figs. 3 and 9).

In practice, we have so far found no samples with a lateral correlation length that is so large that second-order effects have to be considered. It will be interesting to look for such materials to test the applicability of the theory. Specular and nonspecular reflectivity measurements will yield the order of magnitude of rms roughness and lateral correlation length, which will indicate whether second-order effects should be considered. This information is also necessary for a reliable quantification of the compositional depth profile based on GIXRF data.

APPENDIX A: THE SCATTERED FIELD IN AN INTERFACIAL LAYER

We will now consider the field for $n=1$ inside the rough layer at interface j, e.g., for $h_j(\mathbf{x})<z_j<0$. The field is then given by the $i\neq j$ contributions to Eq. (5), plus an $i=j$ contribution amounting to

$$-\frac{1}{4\pi^2}\int\frac{d^2\mathbf{p}_\parallel}{W_p}\exp(i\mathbf{p}_\parallel\cdot\mathbf{x})\int d^2\mathbf{x}'\,\exp[i(\mathbf{k}_\parallel-\mathbf{p}_\parallel)\cdot\mathbf{x}']\bigg[\psi_{\tilde{p}}(z_j)\int_0^{z_j}dz'\,\psi_p(z')V^j\psi_k(z')$$
$$+\psi_p(z_j)\int_{z_j}^{h_j(\mathbf{x}')}dz'\,\psi_{\tilde{p}}(z')V^j\psi_k(z')\bigg].$$

The difference with respect to the field obtained for z_j outside the rough region can be written as $\Delta\phi_{\mathbf{k}}^{(1)}(\mathbf{r})$. We will show that in general this difference may be neglected.

The total field in the interfacial layer can be written as $\phi_{\mathbf{k}}^{(1)}(\mathbf{r})+\Delta\phi_{\mathbf{k}}^{(1)}(\mathbf{r})$, with $\phi_{\mathbf{k}}^{(1)}(\mathbf{r})$ being given by Eq. (5) and

$$\Delta\phi_{\mathbf{k}}^{(1)}(\mathbf{r})=W_k^{-1}\exp(i\mathbf{k}_\parallel\cdot\mathbf{x})\int_0^{z_j}dz'\,V^j[\psi_{\bar{k}}(z_j)\psi_k(z')\psi_k(z')-\psi_k(z_j)\psi_{\bar{k}}(z')\psi_k(z')]$$

$$\simeq(k_{cj}^2-k_{c,j-1}^2)\exp(i\mathbf{k}_\parallel\cdot\mathbf{x})[O(z_j^2)+O(k_jz_j^3)+O(k_j^2z_j^4)].$$

This yields, as a contribution to $T_j^{(2)}(k',k)$ [Eq. (6)],

$$\Delta T_j^{(2)}(k',k)\simeq(k_{cj}^2-k_{c,j-1}^2)^2\int d^2\mathbf{x}\int_0^{h_j(\mathbf{x})}[O(z_j^2)+O(k_jz_j^3)+O(k_j^2z_j^4)]$$

$$=(k_{cj}^2-k_{c,j-1}^2)^2\int d^2\mathbf{x}[O(h_j^3(\mathbf{x}))+O(k_jh_j^4(\mathbf{x}))+O(k_j^2h_j^5(\mathbf{x}))].$$

The configurational average is

$$\langle\Delta T_j^{(2)}(k',k)\rangle\simeq O[A(k_{cj}^2-k_{c,j-1}^2)^2k_j\sigma_j^4].$$

Hence the contribution to the reflectivity, Eq. (17), is

$$\Delta r_k^{(2)}\simeq O[(k_{cj}^2-k_{c,j-1}^2)^2\sigma_j^4],$$

which in general is $\ll 1$.

The same consideration holds for the XRF contributions I_2, where we find a contribution of $O[(k_{cj}^2-k_{c,j-1}^2)^2\sigma_j^4/k_j]$, and I_5, where we find a contribution of $O[k_j(k_{cj}^2-k_{c,j-1}^2)\sigma_j^4]$.

APPENDIX B: DIFFUSE SCATTERING IN THE SECOND-ORDER DWBA

Here we will estimate the order of magnitude of the second-order contribution to diffuse scattering. For the sake of simplicity, we will evaluate the contribution from interface j and will neglect the smaller cross terms between the interfaces.

The leading term of the first-order T matrix, Eq. (10), can be written as

$$T_j^{(1)}(p,k)\simeq(k_{cj}^2-k_{c,j-1}^2)E_j(p)E_j(k)\int d^2\mathbf{x}\,\exp[i(\mathbf{p}_\parallel-\mathbf{k}_\parallel)\cdot\mathbf{x}][h_j(\mathbf{x})+O(k_jh_j^2(\mathbf{x})].$$

This yields a contribution to the diffuse-scattering cross section, Eq. (9), proportional to

$$\langle|T_j^{(1)}(p,k)|^2\rangle\simeq A|k_{cj}^2-k_{c,j-1}^2|^2|E_j(p)|^2|E_j(k)|^2\sigma_j^2\xi_j^2\,\exp[-(\mathbf{p}_\parallel-\mathbf{k}_\parallel)^2\xi_j^2/4]$$

on the assumption of $H_j=1$. For the second-order contribution with $i=j$, Eq. (7) yields

$$T_j^{(2)}(p,k)=-\frac{1}{4\pi^2}\int\frac{d^2\mathbf{p}'_\parallel}{W_{p'}}T_j^{(1)}(p,p')T_j^{(1)}(\overline{p'},k)$$

$$\simeq\frac{(k_{cj}^2-k_{c,j-1}^2)^2}{4\pi^2}E_j(p)E_j(k)\int\frac{d^2\mathbf{p}'_\parallel}{W_{p'}}E_j(p')E_j(\overline{p'})\int d^2\mathbf{x}\int d^2\mathbf{x}'\,\exp[i(\mathbf{p}_\parallel-\mathbf{p}'_\parallel)\cdot\mathbf{x}+i(\mathbf{p}'_\parallel-\mathbf{k}_\parallel)\cdot\mathbf{x}']\{h_j(\mathbf{x})h_j(\mathbf{x}')$$

$$+O[k_jh_j^2(\mathbf{x})h_j(\mathbf{x}')]+O[k_jh_j(\mathbf{x})h_j^2(\mathbf{x}')]\}.$$

This yields a contribution to the diffuse-scattering cross section proportional to $2\,\mathrm{Re}\langle T_j^{(1)*}(p,k)T_j^{(2)}(p,k)\rangle+\langle|T_j^{(2)}(p,k)|^2\rangle$. We find

$$\langle T_j^{(1)*}(p,k)T_j^{(2)}(p,k)\rangle$$

$$\simeq\frac{1}{4\pi^2}|k_{cj}^2-k_{c,j-1}^2|^2(k_{cj}^2-k_{c,j-1}^2)|E_j(p)|^2|E_j(k)|^2\int\frac{d^2\mathbf{p}'_\parallel}{W_{p'}}E_j(p')E_j(\overline{p'})\int d^2\mathbf{x}\int d^2\mathbf{x}'\int d^2\mathbf{x}''\,\exp[i(\mathbf{p}_\parallel-\mathbf{p}'_\parallel)\cdot\mathbf{x}$$

$$+i(\mathbf{p}'_\parallel-\mathbf{k}_\parallel)\cdot\mathbf{x}'-i(\mathbf{p}_\parallel-\mathbf{k}_\parallel)\cdot\mathbf{x}'']\{\langle h_j(\mathbf{x})h_j(\mathbf{x}')h_j(\mathbf{x}'')\rangle+O[k_j\langle h_j(\mathbf{x})h_j(\mathbf{x}')h_j(\mathbf{x}'')^2\rangle]+\cdots\},$$

where $\cdots$ indicates terms with another h_j squared. All these terms contribute to the same order.

Now we will assume that the probability distribution of height deviations at n lateral positions is an n-dimensional Gaussian distribution,[30] implying $\langle h_j(\mathbf{x})h_j(\mathbf{x}')h_j(\mathbf{x}'')\rangle=0$ and

$$\langle h_j(\mathbf{x})h_j(\mathbf{x}')h_j(\mathbf{x}'')h_j(\mathbf{x}''')\rangle=\langle h_j(\mathbf{x})h_j(\mathbf{x}')\rangle\langle h_j(\mathbf{x}'')h_j(\mathbf{x}''')\rangle+\langle h_j(\mathbf{x})h_j(\mathbf{x}'')\rangle\langle h_j(\mathbf{x}')h_j(\mathbf{x}''')\rangle+\langle h_j(\mathbf{x})h_j(\mathbf{x}''')\rangle\langle h_j(\mathbf{x}')h_j(\mathbf{x}'')\rangle.$$

We then obtain

$$\langle T_j^{(1)*}(p,k)T_j^{(2)}(p,k)\rangle=O\Bigg\{k_j|k_{cj}^2-k_{c,j-1}^2|^2(k_{cj}^2-k_{c,j-1}^2)|E_j(p)|^2|E_j(k)|^2\sigma_j^4\int\frac{d^2\mathbf{p}'_\parallel}{W_{p'}}E_j(p')E_j(\overline{p'})$$
$$\times\int d^2\mathbf{x}\int d^2\mathbf{X}\int d^2\mathbf{X}'\ \exp[i(\mathbf{p}_\parallel-\mathbf{p}'_\parallel)\cdot\mathbf{X}+i(\mathbf{p}'_\parallel-\mathbf{k}_\parallel)\cdot\mathbf{X}']\exp[-(\mathbf{X}^2+\mathbf{X}'^2)/\xi_j^2]\Bigg\}.$$

The integral over $\mathbf{x}$ equals the sample area A. The integrals over $\mathbf{X}$ and $\mathbf{X}'$ yield $\tilde{C}_j(\mathbf{p}_\parallel-\mathbf{p}'_\parallel)$ and $\tilde{C}_j(\mathbf{p}'_\parallel-\mathbf{k}_\parallel)$, respectively. If $k_0^2\xi_j/|\mathbf{k}|\gg1$, one of these terms will approach a δ function, yielding

$$\langle T_j^{(1)*}(p,k)T_j^{(2)}(p,k)\rangle=O\Bigg\{Ak_j|k_{cj}^2-k_{c,j-1}^2|^2(k_{cj}^2-k_{c,j-1}^2)|E_j(p)|^2|E_j(k)|^2\,\frac{E_j(k)E_j(\bar{k})}{W_k}\,\sigma_j^4\xi_j^2\,\exp[-(\mathbf{p}_\parallel-\mathbf{k}_\parallel)^2\xi_j^2/4]\Bigg\}.$$

Hence the ratio to the first-order contribution is

$$\langle T_j^{(1)*}(p,k)T_j^{(2)}(p,k)\rangle/\langle|T_j^{(1)}(p,k)|^2\rangle=O[k_j(k_{cj}^2-k_{c,j-1}^2)\sigma_j^2E_j(k)E_j(\bar{k})/W_k].$$

For a single interface the last three factors give $i(k_{j-1}+k_j)^{-1}$ and we have

$$\langle T_j^{(1)*}(p,k)T_j^{(2)}(p,k)\rangle/\langle|T_j^{(1)}(p,k)|^2\rangle=O(E_j^{\uparrow}k_j^2\sigma_j^2).$$

If $k_0^2\xi_j/|\mathbf{k}|\ll1$, the two-dimensional integral over $\mathbf{p}'_\parallel$ is of the order of an angular integral which is approximately $(|\mathbf{k}|\xi)^{-1}$ times a one-dimensional integral over $|\mathbf{p}'_\parallel|$ from $|\mathbf{k}_\parallel|-\xi^{-1}$ to $|\mathbf{k}_\parallel|+\xi^{-1}$, which is of the order $\sqrt{|\mathbf{k}|/\xi}$. The result is $\langle T_j^{(1)*}(p,k)T_j^{(2)}(p,k)\rangle/\langle|T_j^{(1)}(p,k)|^2\rangle=O(k_0\sqrt{\xi_j/|\mathbf{k}|}E_j^{\uparrow}k_j^2\sigma_j^2)$.

In a similar way we can estimate the contribution from $\langle|T_j^{(2)}(p,k)|^2\rangle$. We find

$$\langle|T_j^{(2)}(p,k)|^2\rangle/\langle|T_j^{(1)}(p,k)|^2\rangle=O(|E_j^{\uparrow}|^2k_j^2\sigma_j^2)\quad\text{for }k_0^2\xi_j/|\mathbf{k}|\gg1,$$

$$\langle|T_j^{(2)}(p,k)|^2\rangle/\langle|T_j^{(1)}(p,k)|^2\rangle=O(k_0^2\xi_j/|\mathbf{k}||E_j^{\uparrow}|^2k_j^2\sigma_j^2)\quad\text{for }k_0^2\xi_j/|\mathbf{k}|\ll1.$$

Hence, even if $k_j^2\sigma_j^2$ is appreciable, the second-order contributions may be neglected, except in the case that $k_0^2\xi_j/|\mathbf{k}|\gg1$, and the reflectivity is considerable.

APPENDIX C: REFLECTION AND TRANSMISSION FOR LARGE CORRELATION LENGTHS

In this appendix we will consider a multilayer in which all the interfaces have very large roughness correlation lengths and a very high degree of perpendicular correlation. At a lateral position $\mathbf{x}$, all the interfaces will have the same height deviation $h(\mathbf{x})$ with respect to the position of the smooth interfaces. If compared with the smooth situation, the incident wave field is multiplied by a phase factor $\exp[ik_0h(\mathbf{x})]$, the transmitted wave field in layer j by $\exp[ik_jh(\mathbf{x})]$, and the reflected wave field in layer j by $\exp[-ik_jh(\mathbf{x})]$. Hence, with respect to the incident field, the amplitude for transmission is multiplied by $\exp[i(k_j-k_0)h(\mathbf{x})]$ and the amplitude for reflection by $\exp[-i(k_j+k_0)h(\mathbf{x})]$. If h is a Gaussian random variable with a standard deviation σ, we obtain a factor $\exp[-(k_0-k_j)^2\sigma^2/2]$ for transmission and a factor $\exp[-(k_0+k_j)^2\sigma^2/2]$ for reflection. In particular, for $j=0$, the reflection coefficient of the whole multilayer is multiplied by a factor $\exp(-2k_0^2\sigma^2)$.

[1] D. K. G. de Boer, Phys. Rev. B **44**, 498 (1991).
[2] D. K. G. de Boer, W. W. van den Hoogenhof, and A. J. G. Leenaers, X-Ray Spectrom. **24**, 91 (1995).
[3] D. K. G. de Boer, Phys. Rev. B **49**, 5817 (1994).
[4] D. K. G. de Boer, Phys. Rev. B **51**, 5297 (1995).
[5] S. K. Sinha, E. B. Sirota, S. Garoff, and H. B. Stanley, Phys. Rev. B **38**, 2297 (1988).
[6] V. Holý, J. Kuběna, I. Ohlídal, K. Lischka, and W. Plotz, Phys. Rev. B **47**, 15 896 (1993); V. Holý and T. Baumbach, *ibid.* **49**, 10 688 (1994); V. Holý, J. Kuběna, W. W. van den Hoogenhof, and I. Vávra, Appl. Phys. A **60**, 93 (1995).
[7] S. Dietrich and A. Haase, Phys. Rep. **260**, 1 (1995).
[8] L. S. Rodberg and R. M. Thaler, *Introduction to the Quantum Theory of Scattering* (Academic, New York, 1967).
[9] In Ref. 3 we made a mistake, taking the integration limits $|\mathbf{p}_\parallel|<|\mathbf{k}|$. The integration should be extended to ∞. This does not

affect the rest of the paper: The limiting cases remain the same, and we checked that the numerical results are not distinguishable from those presented.

[10] M. Born and E. Wolf, *Principles of Optics*, 5th ed. (Pergamon, Oxford, 1975).

[11] L. G. Parratt, Phys. Rev. **95**, 359 (1954).

[12] M. K. Sanyal, S. K. Sinha, A. Gibaud, S. K. Satija, C. F. Majkrzak, and H. Homa, in *Surface X-Ray and Neutron Scattering*, edited by H. Zabel and I. K. Robinson (Springer-Verlag, Berlin, 1992), p. 91; S. K. Sinha, J. Phys. (France) III **4**, 1543 (1994).

[13] E. Spiller, D. Stearns, and M. Krumrey, J. Appl. Phys. **74**, 107 (1993).

[14] G. Palasantzas and J. Krim, Phys. Rev. B **48**, 2873 (1993); G. Palasantzas, *ibid*. **48**, 14 472 (1993).

[15] D. K. G. de Boer, A. J. G. Leenaers, and W. W. van den Hoogenhof, Appl. Phys. A **58**, 169 (1994); D. K. G. de Boer, A. J. G. Leenaers, and R. M. Wolf, J. Phys. D **27**, A227 (1995).

[16] J.-P. Schlomka, M. Tolan, L. Schwalowsky, O. H. Seeck, J. Stettner, and W. Press, Phys. Rev. B **51**, 2311 (1995).

[17] L. Névot and P. Croce, Revue Phys. Appl. **15**, 761 (1980).

[18] B. Vidal and P. Vincent, Appl. Opt. **23**, 1794 (1984).

[19] D. K. G. de Boer and A. J. G. Leenaers, Physica B (to be published).

[20] J. M. Eastman, Phys. Thin Films **10**, 167 (1978).

[21] A. Caticha, in *Physics of X-Ray Multilayer Structures, 1994*, Technical Digest Series, Vol. 6 (Optical Society of America, Washington, D.C., 1994), p. 56; Phys. Rev. B **52**, 9214 (1995).

[22] I. A. Artioukov and I. V. Kozhevnikov, Proc. SPIE **2453**, 154 (1995).

[23] W. Weber and B. Lengeler, Phys. Rev. B **46**, 7953 (1992).

[24] M. Kopecky, J. Appl. Phys. **77**, 2380 (1995). The approach followed in this paper seems to be hybrid, mixing expressions for flat and graded interfaces.

[25] V. Holý (private communication).

[26] The width of this region is taken equal to $2\sigma_j$ or 0.4 times the x-ray standing-wave period ($\simeq k_0^{-1}$), whichever is smaller. For large values of k_j, we did not include an interfacial region, but simply used the NC factors.

[27] This discussion complements that given in Ref. 4 (note 18).

[28] M. Tolan and D. Bahr (private communication) demonstrated this for the first time.

[29] To calculate $r_k^{(2)}$, Eq. (19) has to be evaluated. The integral in this formula contains a contribution due to parallel wave vectors greater than $|\mathbf{k}|$, i.e., with imaginary perpendicular wave vector. In practice, this contribution is very small. We found that our scheme fails for an imaginary perpendicular wave vector and decided to use the original fields under these circumstances.

[30] R. Kubo, M. Toda, and N. Hashitsume, *Statistical Physics II, Nonequilibrium Statistical Mechanics*, 2nd ed. (Springer-Verlag, Berlin, 1991), Sec. 1.4.